Energy, Mines and Resources Canada | Énergie, Mines et Ressources Canada

CANMET

Canada Centre for Mineral and Energy Technology | Centre canadien de la technologie des minéraux et de l'énergie

CALIBRATION OF THE NFOLD DISPLACEMENT DISCONTINUITY MODEL OF THE "A" ZONE AT CAMPBELL RED LAKE MINE

D.S.G. HANSON

ELLIOT LAKE LABORATORY

AUGUST 1986

This document is an unedited interim report prepared primarily for discussion and internal reporting purposes. It does not represent a final expression of the opinion of the Canada Centre for Mineral and Energy Technology (CANMET)

Ce document est un rapport provisoire non révisé et rédigé principalement en vue de discussion et de documentation interne. Il ne représente nullement l'opinion définitive du Centre canadien de la technologie des minéraux et de l'énergie (CANMET)

MICROMEDIA

MINING RESEARCH LABORATORIES
DIVISION REPORT MRL 87-36(TR)

CALIBRATION OF THE NFOLD DISPLACEMENT DISCONTINUITY MODEL OF THE "A" ZONE AT CAMPBELL RED LAKE MINE

by

D.S.G. Hanson*

ABSTRACT

The Campbell Red Lake "A" zone has experienced rockburst activity for approximately the last twenty years. Previous NFOLD modelling completed by Golder Associates on the "F" and "F-2" zones suggested calibration of the NFOLD model to the "A" zone. Visual observations documented since 1965 and microseismic observations are combined with elastic and non-elastic yielding applications of NFOLD to the present "A" zone geometry. Analyses are completed with and without the presence of backfill to verify the model/predictions versus actual failure conditions observed by mine personnel.

The calibrated NFOLD model indicates two failure growth patterns observed in the mine, displays a similar extent of failure to that observed underground, and in some cases demonstrates the stabilizing effect of backfill on boxhole/sill pillars. Stress levels of about 100 MPa appear to be critical for the boxhole pillars with successively higher critical stresses necessary for more confined portions of sill pillars and abutments. Many of the boxhole/sill pillars reveal a high extraction geometry, and are extremely meta-stable, indicating the possibility of an on-going chain reaction propagation of failure. Vertical pillars appear generally quite stable.

Keywords: Numerical modelling; Model calibration; Failure patterns.

*Ground Control Engineer, Elliot Lake Laboratory, CANMET, Energy, Mines and Resources Canada, Elliot Lake, Ontario.

ETALONNAGE DU MODÈLE NFOLD DU DÉPLACEMENT DE LA DISCONTINUITÉ DE LA ZONE A DE LA MINE CAMPBELL RED LAKE

par

D.S.G. Hanson

RÉSUMÉ

Depuis les vingt dernières années des coups de toit se produisent dans la zone "A" de Campbell Red Lake. Au cours des travaux réalisés par Golder Associates sur la modélisation NFOLD des zones "F" et "F-2", on a proposé d'effectuer l'étalonnage du modèle NFOLD de la zone "A". Les données recueillies à partir d'observations visuelles depuis 1965 et celles des observations microsismiques ont été combinées aux données du modèle NFOLD des applications de l'affaisement élastique et non élastic de la géométrie actuelle de la zone "A". On a en outre effectué des analyses avec et sans la présence de remblais afin de vérifier les prédictions du modèle par rapport aux conditions réeles de rupture observées par le personnel de la mine.

Le modèle NFOLD étalonné a montré deux modèles d'effondrement en développement déjà observé dans la mine, a illustré aussi l'étendue de l'effondrement tel que remarqué lors des observations souterraines, et dans certains cas a démontré l'effet stabilisateur du remblai sur les piliers de point de soutirage et les piliers de fond. Les niveaux de tension s'élevant à environ 100 MPa semblent critiques pour les piliers de point de soutirage et des tensions critiques progressivement plus elevées sont nécessaires pour les parties confinées des piliers de fond et des centreforts. Plusieurs piliers de point de soutirage et de fond révèlent une géométrie d'extraction élevée et sont extrèmement meta-stable, indiquant la possibilité d'une réaction de propagation de l'effondrement à la chaîne. Les piliers verticaux s'avèrent généralement assez stable.

MOTS-CLÉS: Modélisation numérique, étalonnage de modèle, configuration de l'effondrement.

* Ingénieur de contrôle du sol, Laboratoire d'Elliot Lake, CANMET, Énergie, Mines et Ressources Canada, Elliot Lake, Ontario.

CONTENTS

	Page
ABSTRACT	i
RESUME	ii
INTRODUCTION	1
PURPOSE OF WORK	1
DESCRIPTION OF THE A, A-1 ZONES AND ROCKBURST HISTORY	1
DESCRIPTION OF THE NFOLD PROGRAM	2
INPUT PARAMETERS - NFOLD	6
DESCRIPTION OF THE COARSE NFOLD MINE MODEL	8
Results of Analyses - Coarse Model	12
Interpretation of Results - Coarse NFOLD Model	18
DESCRIPTION OF THE NFOLD 'WINDOW' MODEL - ELASTIC CONDITIONS	19
Results of Analyses - Elastic Window	19
Interpretation of Results - Elastic Window	21
DESCRIPTION OF THE NFOLD 'WINDOW' MODEL - YIELDING CONDITIONS	23
Results of the Analyses - Yielding Window	25
Interpretation of Results - Yielding Window	31
DESCRIPTION OF THE COARSE NFOLD MINE MODEL AND WINDOW INCORPORATING BACKFILL	32
Results of the Analyses - Window	32
Interpretation of the Results for Models Incorporating Backfill	37
MINE STIFFNESS	39
CONCLUSIONS	41
ACKNOWLEDGEMENTS	43
REFERENCES	43

TABLES

No.		
1.	Previous rockbursts at Campbell Red Lake Mine - "A" zone	3
2.	Evaluation of field stresses Campbell Red Lake Mine	7
3.	Load/deformation properties - "A" and "A-1" zone (backfill included)	26

FIGURES

1.	Former sequential rockburst locations at the Campbell Red Lake Mine - "A" zone	5

No.		Page
2.	Coarse NFOLD model and windows	10
3.	Cross-sectional view of coarse NFOLD layout for "A" zone Campbell Red Lake Mine	11
4.	Elastic conditions, no backfill - normal stresses, "A" zone	13
5.	Elastic conditions, no backfill - normal stresses, "A-1" zone	14
6.	Elastic conditions, no backfill - convergence, "A" zone	16
7.	Elastic conditions, no backfill - convergence, "A-1" zone	17
8.	Elastic conditions, no backfill - normal stress, window "A" zone.	20
9.	Elastic conditions, no backfill - convergence window, "A" zone	22
10.	Load deformational behaviour of the various yielding elements c/w backfill elements assigned to the NFOLD model	24
11.	Yielding conditions, no backfill - normal stresses, window "A" zone	27
12.	Yielding conditions, no backfill - factor of safety, window, "A" zone	28
13.	Yielding conditions, no backfill - convergence window "A" zone	29
14.	Yielding conditions with backfill - mining pattern yield areas, window "A" zone	33
15.	Yielding conditions with backfill - normal stresses, window "A" zone	34
16.	Yielding conditions with backfill - factor of safety, window "A" zone	35
17.	Yielding conditions with backfill - convergence, window "A" zone.	38

INTRODUCTION

This report describes the set-up and initial results of the computer stress models using Golder Associates NFOLD computer program for the Campbell Red Lake Mines in Ontario. Models of the "A" and "A-1" zones were completed during June 1986 at the Elliot Lake Mining Research Laboratory.

PURPOSE OF WORK

The intent of this report is to be supplementary to the work carried out at Campbell Red Lake Mines (1), and Golder Associates (2) during September 1985.

This report goes somewhat further in attempting to calibrate the NFOLD model to the "A" and "A-1" zones incorporating the presence of backfill in the mining stopes.

DESCRIPTION OF THE A, A-1 ZONES AND ROCKBURST HISTORY

The "A" and "A-1" zones are two of several ore zones present within the Campbell deposit. These zones strike northwest and dip 75-80^{o} to the southwest, and are contained within the mafic-ultramafic meta-volcanics. Within the "A" zone mining by overhead shrinkage down to the 1002 level was followed by the cut-and-fill method below using hydraulically placed mine tailings. More recent mining of the "A-1" zone has involved the same cut-and-fill method.

Most of the early rockburst activity occurred in the shrinkage stopes while attempting to recover the sill pillars. Those events have been reasonably well documented since 1965, both through visual observation and later through microseismic source location.

Those events of a violent failure occurred when the "A" zone geometry

was much different from today. A sequential account is shown in both Table 1 and Figure 1.

The occurrence of these bursts was due to the high degree of extraction in the Campbell Red Lake "A" zone, and possibly the presence of the mine workings in the adjacent Dickenson Mine (Figure 1).

For the most part the following observations can be made:

a) the rockbursts were nearly exclusively confined to the boxhole pillars;

b) two types of failure sequences were observed: (i) the west and east extremities of a boxhole/sill pillar combination failed first sequentially migrating towards the centre, or (ii) the rockburst failure migrated from east to west along a boxhole/sill pillar;

Examination of the high degree of extraction when looking at a longitudinal section of the mine suggests the possibility of pillar bursting, especially as the host rock has been described as being extremely brittle.

DESCRIPTION OF THE NFOLD PROGRAM

NFOLD is a three-dimensional displacement discontinuity, stress and displacement analytical method. It is more advanced than the similar DZTAB program in that it can incorporate not only elastic, but post-failure properties as well.

In the modelling completed on the "A" and "A-1" zones the individual elements were rectangular rather than square as was the case of older NFOLD program models.

For the elements incorporated in the model, the loading modulus, peak strength, unloading modulus, and residual strengths are specified according to the extent of confinement. Those elements near the immediate stope opening are assigned lower strengths compared to those further into the rock mass.

Failure is simulated as the strength of a particular element is

Table 1 - Previous rockbursts at Campbell Red Lake Mine - "A" zone

Location	Year	Date	Sequence
502E Crown	1965	Feb. 7	1
" "		Feb. 16	2
602E Sill		April 28	3
902E Sill		June 19	4
1002E Sill		July 2	5
602E Sill	1966	Sept. 27	6
602 702E Sills		Nov. 1-3	7
1002E Sill	1967	April 28	8
702E Sill		June 24	9
1002E Sill		July 11	10
802E Sill	1970	April 20	11
802E Sill		May 15	12
802E Sill		Nov. 18	13
702,802E Crown	1971	Jan. 9-10-11	14
802E Sill		Jan. 15	15
802E Sill		Jan. 19	16
1002E Sill		Jan. 26	17
802E Sill		Feb. 4	18
802E Sill		Feb. 8-9	19
702E Sill	1972	April 3	20
702E Sill		June 19	21
1002E Sill	1975	Mar. 11	22
1002E Sill	1976	Feb. 7	23
1002E Sill		June 17-30, Aug. 23	24
802E Crown	1977	May 19	25
702E Sill		Sept. 15	26
702E Sill		Nov. 2	27
1002E Sill	1978	Nov. 28	28
1002E Sill	1980	May 7-12	29
1002E Sill	1981	May 14	30
902E Drift	1986	March 29	31
1002E Drift		March 29	32
[illegible]E Drift		March 29	33
1002E Drift		March 29	34
902E Drift		March 29	35
1002E Drift		March 29	36
1002E Drift		March 29	37
902E Drift		March 29	38
502E Drift		March 29	39
702E Drift		March 29	40
902E Drift		March 30	41
902E Drift		March 30	42
1002E Drift		March 31	43

Cont. overleaf

Table 1 - Continued

Location	Year	Date	Sequence
602E Drift	1986	April 1	44
602E Drift		April 1	45
902E Drift		April 7	46
802E Drift		April 7	47
902E Drift		May 4	48
702E Drift		May 26	49
702E Drift		May 26	50
1002E Drift		June 5	51
702E Drift		July 30	52
902E Drift		July 30	53
702E Drift		July 30	54
802E Drift		July 30	55
402E Drift		July 30	56
702E Drift		July 31	57
602E Drift		August 2	58
602E Drift		August 3	59
602E Drift		August 3	60
602E Drift		August 3	61
602E Drift		August 15	62
602E Drift		August 15	63
402E Drift		August 15	64
402E Drift		August 15	65
602E Drift		August 20	66
502E Drift		August 20	67
602E Drift		August 20	68
602E Drift		August 22	69
402E Drift		August 23	70
302E Drift		August 23	71

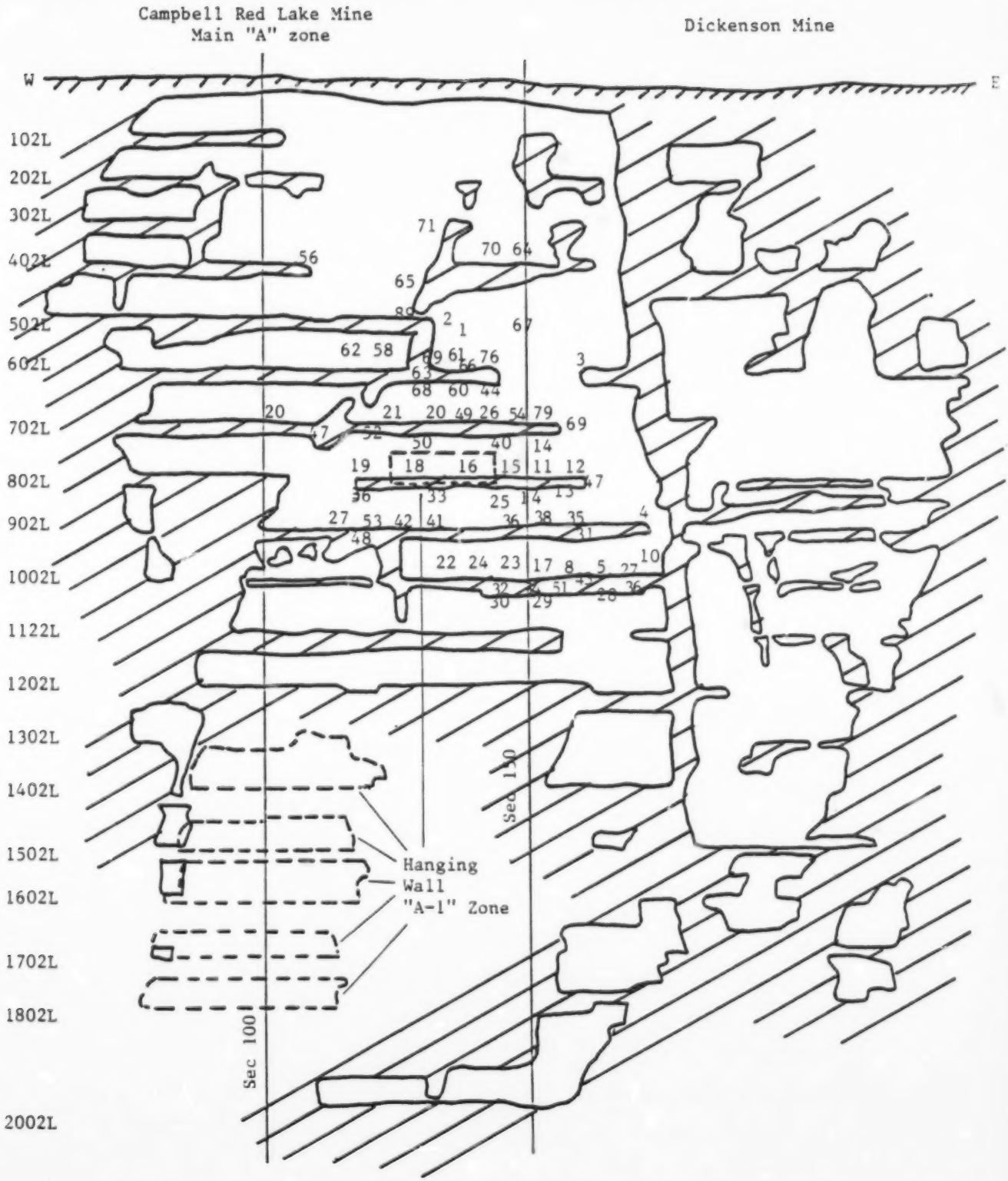

Fig. 1 - Former sequential rockburst locations at the Campbell Red Lake Mine - "A" zone.

exceeded, resulting in stress transfer to the more competent elements which have not failed. Failure growth can, therefore, be simulated as well. The model is said to be calibrated when the degree of failure predicted for a mining geometry is in reasonable agreement with the actual degree of failure witnessed at the mine for the same geometry.

The procedure in general is to model a particular mining geometry using elastic properties assigned to the model elements representing the unmined portions of the rock mass, until the onset of failure. A small degree of mining from this point on will therefore result in more failure. These stress conditions are used as an estimate of the failure strength of elements in, or near, the known failed areas.

Post failure elements are then incorporated in the mined geometry at the onset of failure with various load-deformational properties assigned according to their degree of confinement. Here the weaker elements fail and transfer stress over to the stronger elements (having higher confining stress).

Adjustments in the assigned element peak strengths are carried out until the observed and predicted results agree favourably. This exercise is known as calibrating or 'fine tuning' the model for future mining strategy. As a result future mining 'scenarios' can be evaluated effectively once the model's predictability has been verified.

INPUT PARAMETERS - NFOLD

The in situ field stress measurements were taken by CANMET's Elliot Lake Laboratory (3). Table 2 shows the results of the Campbell Red Lake data in relation to a percentage differential with other Northern Ontario data.

The following input data was used in the NFOLD model:

Modulus of deformation 69000 MPa

Table 2 - Evaluation of field stresses, Campbell Red Lake Mine.
(B. Arjang)

Depth Below Surface	Test No.	Field Stresses (in MPa), CRL Mine σ_1 Brg./Dip	σ_2 Brg./Dip	σ_3 Brg./Dip	σ_V % Diff.[x]	σ_{Ha} % Diff.	σ_{Ha}/σ_V % Diff.	Northern Ontario Data* (MPa)
625 m	CRL T1-2	23	15	10	14	19	1.4	σ_V=16, σ_{Ha}=33
(14 L)	CRL T1-3	060°/40°	214°/33°	134°/33°	12%	42%	6%	σ_{Ha}/σ_V=1.5
	combined							
990 m	3 test	53	24	12	25	38	1.5	σ_V=26, σ_{Ha}=44
(22 L)	combined	087°/16°	322°/57°	185°/26°	4%	13%	7%	σ_{Ha}/σ_V=1.4
1220 m	CRL T3-2	70	41	31	34	55	1.6	σ_V=32, σ_{Ha}=47
(27 L)	CRL T3-3	230°/10°	020°/76°	140°/07°	6%	17%	14%	σ_{Ha}/σ_V=1.4
	combined							

[x] Differences of vertical (σ_V), average horizontal (σ_{Ha}) stresses and stress ratio (σ_{Ha}/σ_V) with Northern Ontario data.

* Northern Ontario data, obtained from stress gradients in the Canadian Shield (7,8) defined as:

σ_V = 0.027 MPa/m (obtained from overburden weight).

σ_{Ha} = 9.86 MPa + 0.0371 MPa/m (0-900 m depth below surface).

σ_{Ha} = 33.41 MPa + 0.0111 MPa/m (900-2200 m depth below surface).

$$\sigma_{Ha}/\sigma_V = \frac{251.68}{\text{depth m}} + 1.14$$

Poisson's Ratio 0.2

For the primitive stress components in relation to the orebody the assignments were:

BXX (horizontal stress perpendicular) = 0.046 MPa/m depth

BYY (horizontal stress parallel) = 0.027 MPa/m depth

BZZ (vertical stress) = 0.027 MPa/m depth

The shear stresses BXY, BXZ, and BYZ were assigned zero values as the in situ field stress measurements recorded near zero strain values.

As no stress measurements had been taken near surface, the following stress components representing the intercept at surface were assigned zero values.

AXX = AYY = AZZ = 0.0 and AXY = AYZ = AZX = 0.0

where, σ_{XX} = AXX + BXX.Z

σ_{YY} = AYY + BYY.Z

σ_{ZZ} = AZZ + BZZ.Z

σ_{XY} = AXY + BXY.Z

σ_{YZ} = AYZ + BYZ.Z

σ_{XZ} = AXZ + BXZ.Z

Previous NFOLD models completed by Golder Associates, Vancouver did assume the same values for the Z = 0 (depth below surface) intercept.

The stress measurements were taken from the "F", "G" and "L" zones at Campbell Red Lake Mines.

In order to compare the former modelling results with the current, input parameters were changed only if the new data suggested considerable differences.

DESCRIPTION OF THE COARSE NFOLD MINE MODEL

The NFOLD model was considered appropriate for modelling the "A-1" and

"A" zones as both are tabular orebodies of reasonably consistent strike, dip and thickness. In particular, the zone thicknesses are small in relation to their other orebody dimensions. The capability of the model to include multiple folds allowed the superimposition of the "A-1" hanging wall zone on the main "A" zone.

Analysis of the "A" and "A-1" zones involved a series of various modelling runs using the following format:

a) The "A" and "A-1" zones were modelled elastically covering an areal expanse as shown in Figures 2 and 3. The mining pattern, perpendicular stress and convergence output files were examined.

b) A windowed portion of the "A" zone through the "SCALNF" option (Figure 2) was completed, and again an elastic analysis involving inspection of mining pattern, perpendicular stress and convergence output files.

c) Analysis of the 'window' on the "A" zone using yielding elements to account for post-failure behaviour was completed, and observations concerning mining pattern, failure areas, perpendicular stress, convergence, and factors of safety examined.

d) The above three routines were followed through once more incorporating the effects of backfill as a stabilizing medium in improving the general ground conditions in the mine.

The initial coarse mine model was established as shown in Figure 2 and 3. This resulted in 14 joints being created on strike for the "A" and "A-1" zones, 30 limbs down dip for the "A" zone, and 17 limbs down dip for the "A-1" zone. The above structure resulted in a total of (14 x 47 x 25) 16,450 elements having dimensions of 12.18 m on strike and 6.10 m down dip. An earlier coarse run failed to execute as it had exceeded the 50 combined limb limit now assigned to the current NFOLD program capability.

The dip of the orebody was assumed to be 80^{o} with a thickness of 2.0 m

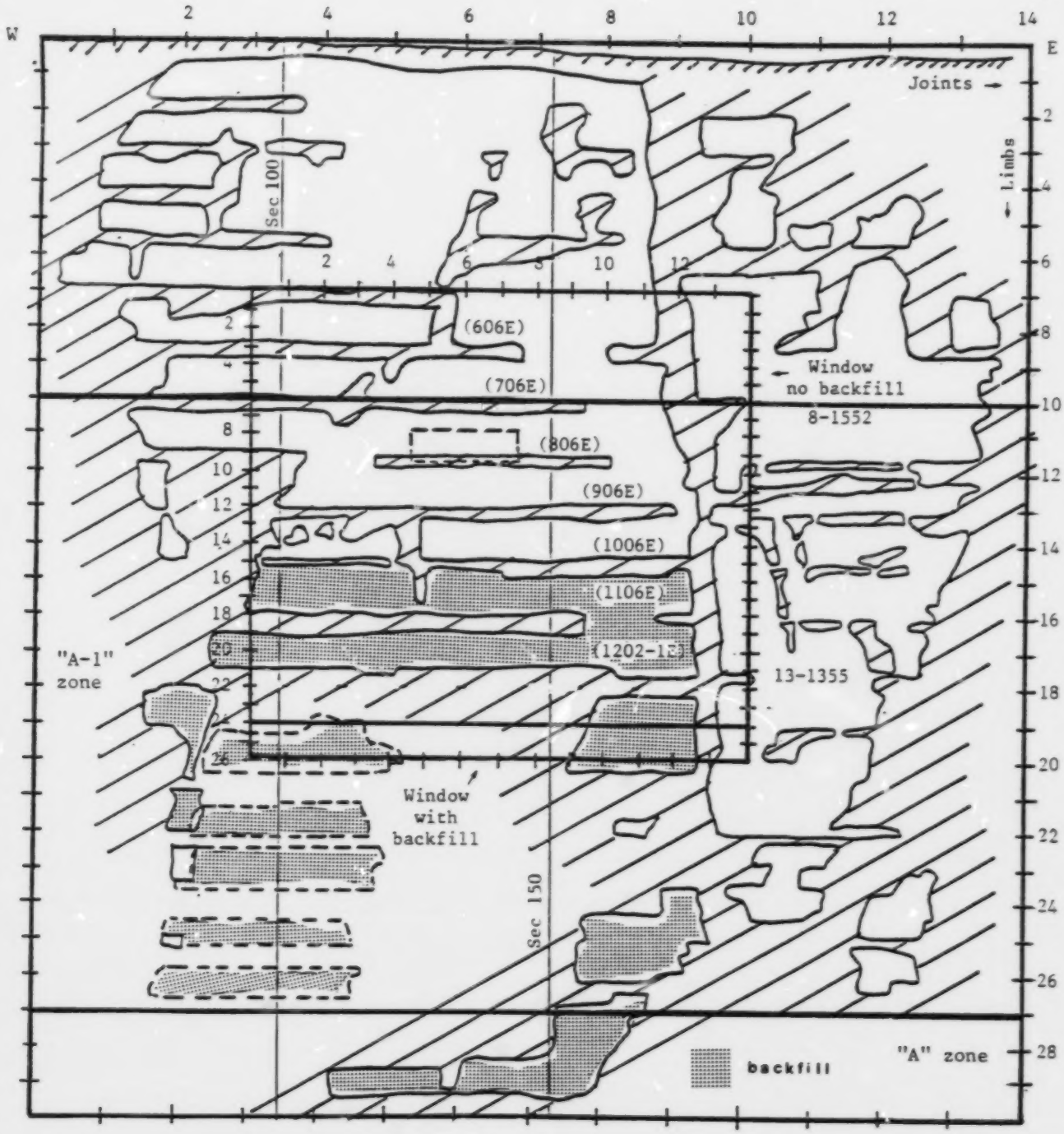

Fig. 2 - Coarse NFOLD model and windows.

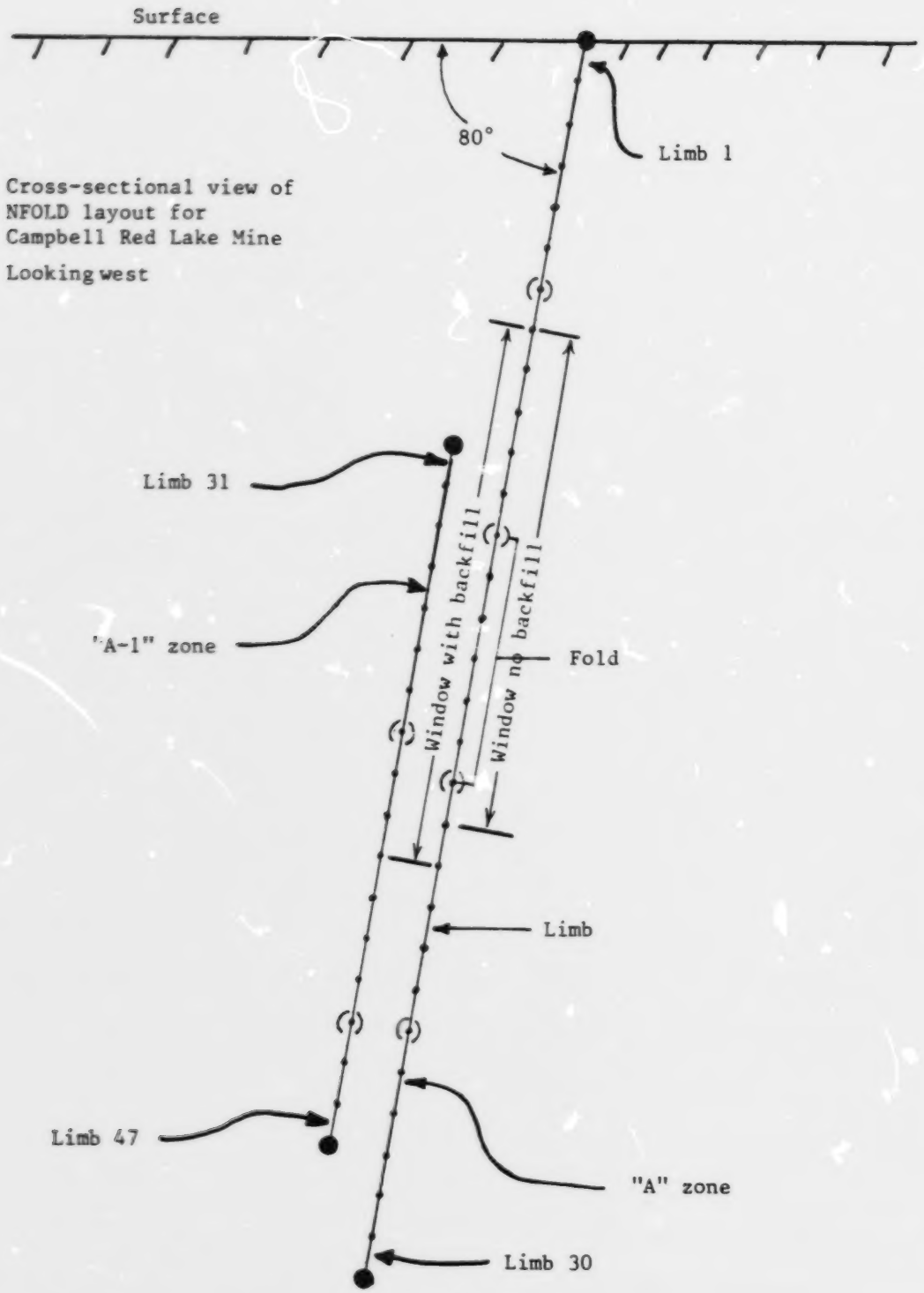

Fig. 3 - Cross-sectional view of coarse NFOLD layout for "A" zone Campbell Red Lake Mine.

measured from hanging wall to footwall.

RESULTS OF ANALYSES - COARSE MODEL

The coarseness of scale of the large 12.18 by 6.10 m elements did not allow accurate modelling of the boxhole pillars on each level so these pillars were modelled as solid crown pillars, as had been done in the past "F" zone models. As the element dimensions were smaller in the down dip direction than horizontally, the printer plots for all output are stretched which distorts the vertical dimensioning of the mine geometry.

Figures 4 and 5 show the perpendicular stress levels for the elastic analysis of the "A" and "A-1" zones. The stress levels reflect elastic unmined portions where failure was not allowed to occur. Consequently, some stress levels are very high, and in actual fact would have failed.

The effect of the previously mined "A" zone on the perpendicular stress levels experienced in the "A-1" zone is evident by the stress shadowing in Figure 5. Stress levels are maintained at, or are slightly higher than, the virgin perpendicular values for the same depth along the barrier pillar (Joint 10, limbs 31-45), but on either side of the pillar there is compressive stress reduction. The reduction seems more prevalent opposite those areas (1402-1, 1206-1106, 13-1355, 8-1552 stopes) where the areal exposure is greatest. If any future stopes ("A-1" zone) were to be considered in the reduced stressed regions, these future stoping blocks would benefit as normal stresses would probably be fairly low with reduced stress related problems.

For the "A" zone, the only sill pillar that appears to be highly stressed is the 806E pillar (Figure 4). Stresses are reasonably high in the east end of the 1106, 1206 sills, and western portions of the Dickenson Mine appear to be extremely highly stressed due mainly to the high degree of extraction.

The presence of the small "A-1" stope above the 804 level has reduced

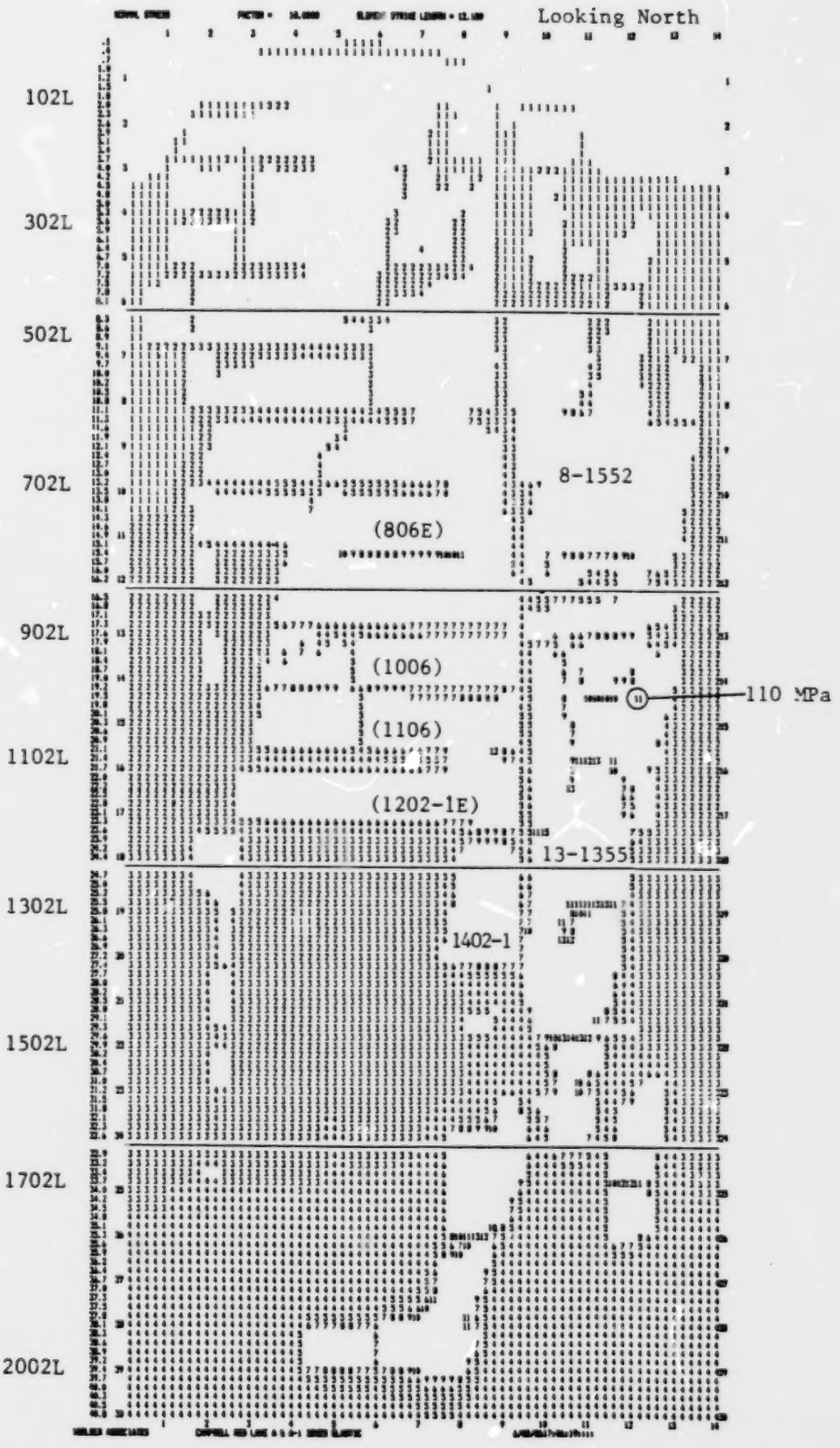

Fig. 4 - Elastic conditions, no backfill - normal stresses, "A" zone.

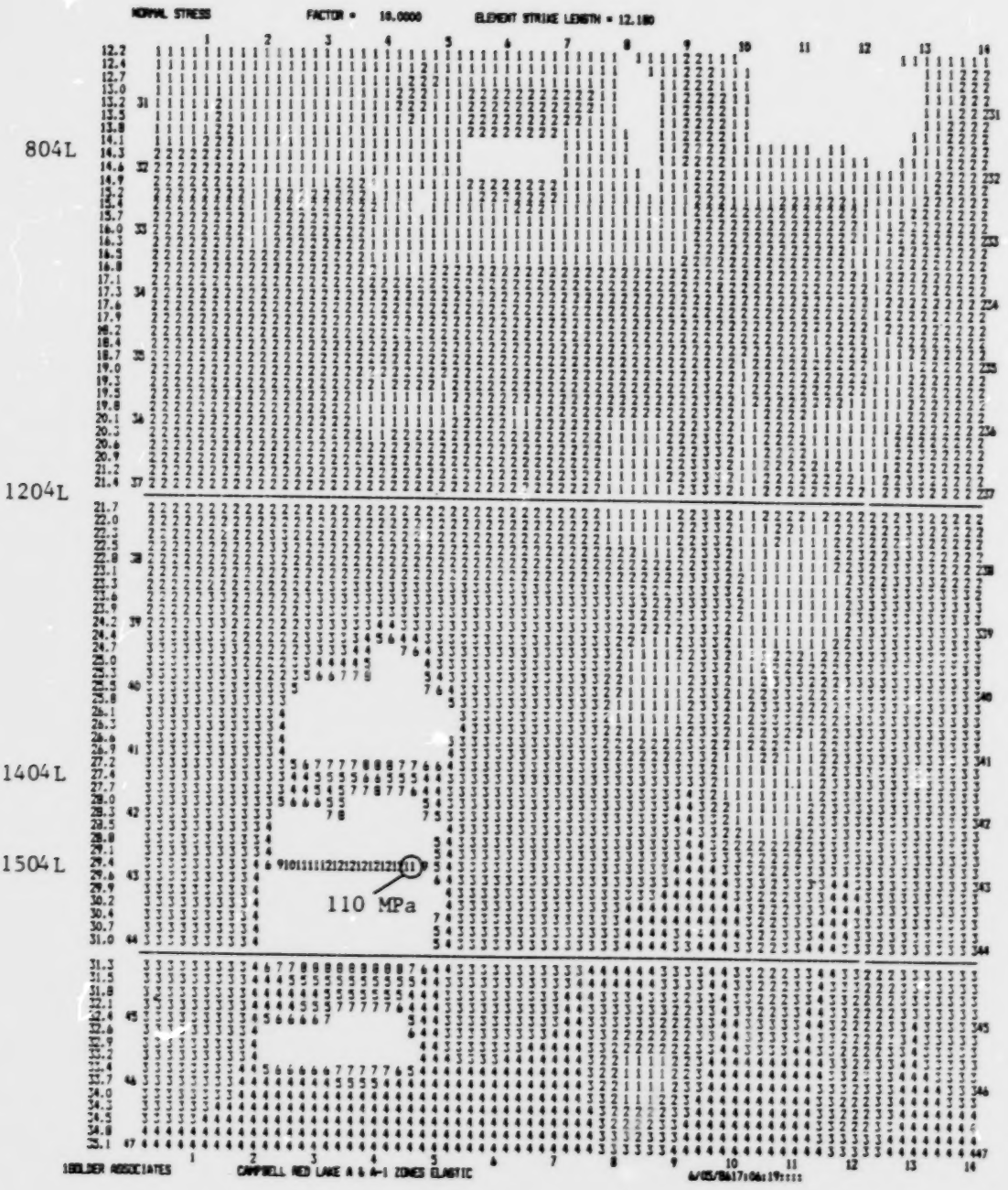

Fig. 5 - Elastic conditions, no backfill - normal stresses, "A-1" zone.

stresses within the central core of the 806E pillar in the "A" zone, but has streamlined stresses around its east and west extremities to increase the perpendicular stresses to both east and west ends of the 806E sill pillar. The stress reduction, however, has only been slight.

The 806E pillar stress response does not reflect the mine sequencing history of the 806E pillar in relation to the overall mine geometry. In actual fact, the perpendicular stresses in the central core were probably higher than indicated, and the east and west extremities somewhat lower, as the "A" zone had been mined out years before the "A-1" zone geometry's influence in this immediate area.

The 1502 sill in the "A-1" zone appears to have high enough stresses to suggest that pillar failure could occur. In other sills the ore is much too wide at the moment to be experiencing failure.

Figures 6 and 7 reveal the type of convergence expected assuming no fill is present in the stopes. Convergence is incorporated into the analysis as the source of rock bursting is due, not only to the stress levels within the unmined elements within the ore seam, but the potential energy of the wall rocks as well. Also, in order to compare the positive effects of the presence of backfill in the stopes in providing confinement to the stope walls, it is necessary to examine the convergence of the walls of stopes first without backfill and then with backfill to see the net effect.

Figure 7 also shows that some divergence in the areas of the reduced perpendicular stress shadows has occurred. The influence of the "A" zone on the "A-1" zone has caused stress reductions in several locations, but the reverse is not true. A possible explanation is that the "A-1" zone's limited areal extent results in a much reduced influence on the "A" zone. The convergence results support this relationship.

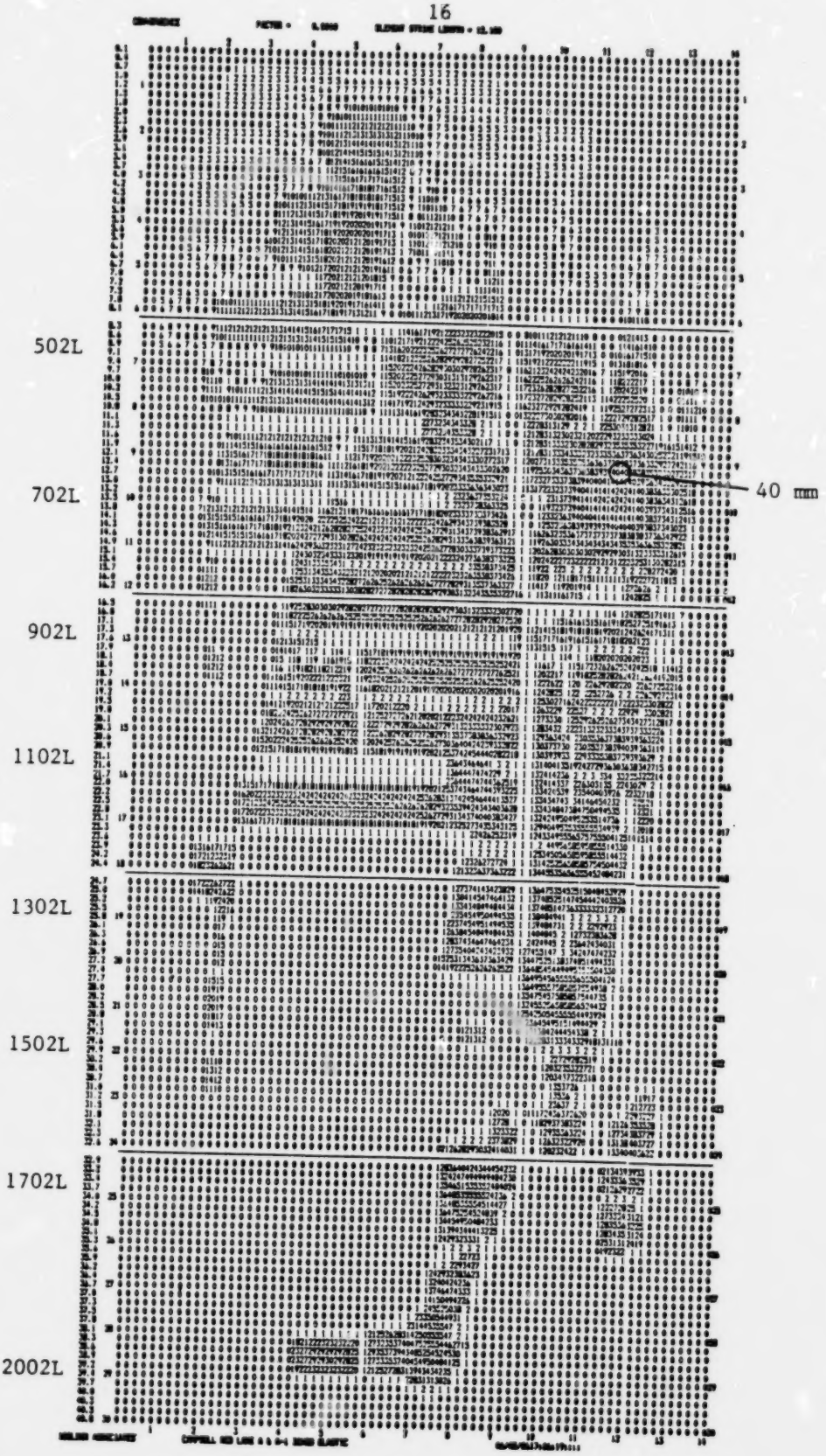

Fig. 6 - Elastic conditions, no backfill - convergence, "A" zone.

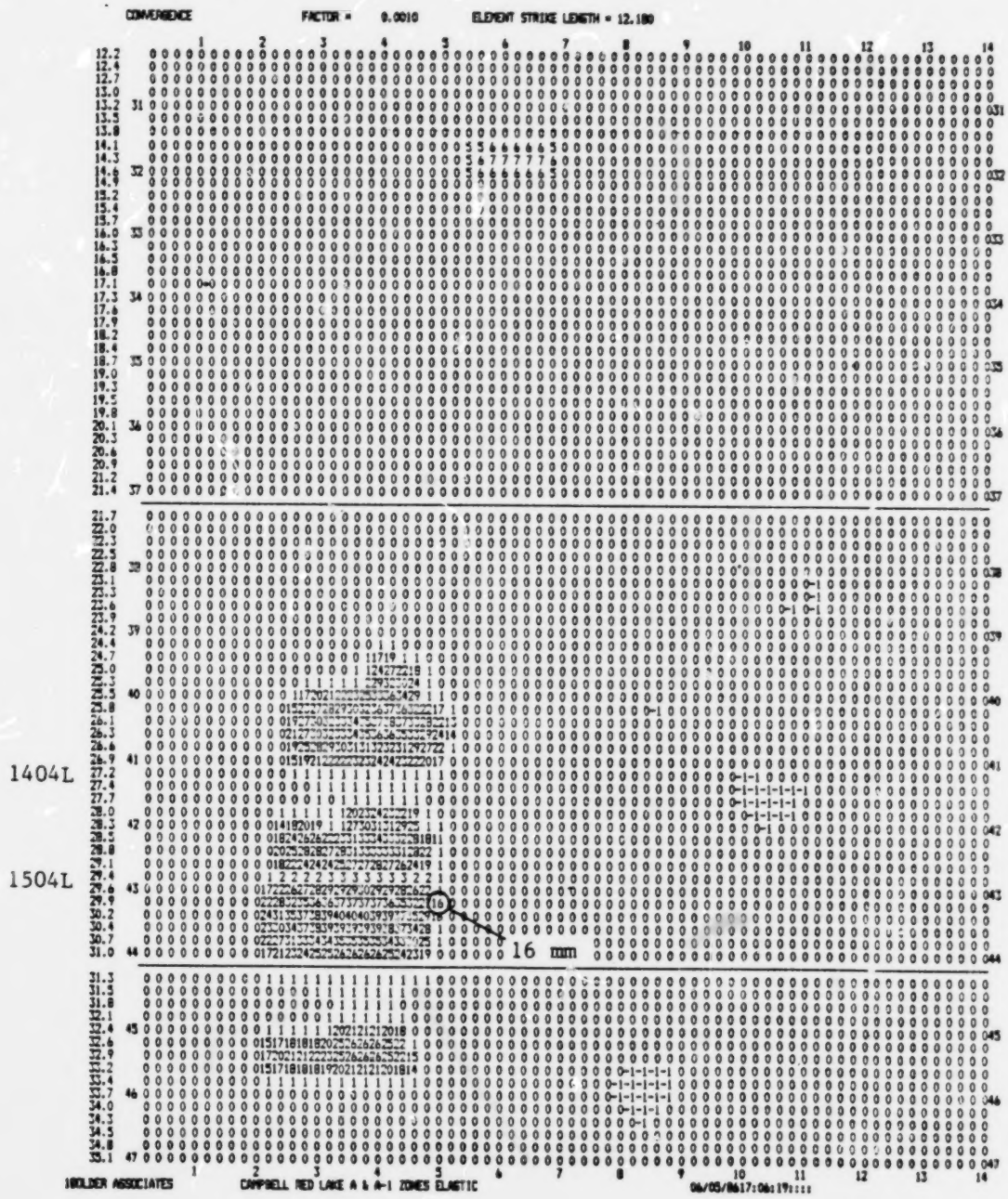

Fig. 7 - Elastic conditions, no backfill - convergence, "A-1" zone.

INTERPRETATION OF RESULTS - COARSE NFOLD MODEL

Since the coarse mine model was run elastically it does not produce failure conditions. It does, however, allow one to examine the areas where failure has occurred in the mine and the stresses that correspond to a purely elastic situation. In this way an approximate value of yield strength is provided.

Stress shadowing results when one ore seam is mined prior to the other. The amount of perpendicular stress reduction in overlapping ore seams is directly proportional to the degree of extraction of one seam versus the other, or the amount of overlapping that occurs. However, the degree of stress reductions for the two seams is not mutually exclusive.

For the same depth below surface the vertical pillars are more stable than their horizontal counterparts. In most cases the vertical pillar strike length exceeds the sill pillar dip width.

For sill and crown pillars that are isolated from the rock mass (island effect), both the east and west extremities are the highest stressed. For those sill and crowns that are linked to neighbouring vertical pillars, or to the west abutment the stresses are generally higher next to the Dickenson boundary. The above effects seem logical to what one would expect.

On either side of the boundary pillar separating Campbell Red Lake Mines and Dickenson Mines small sill pillar remnants are very highly stressed and probably have failed.

The coarseness of the model does not allow adequate modelling of the boxhole pillars as the individual element size reduces its sensitivity to intricate mine geometry.

The importance of examining convergence is not that apparent at this stage of the analysis, but is something that must be considered when accounting for the stabilizing effect of backfill.

DESCRIPTION OF THE NFOLD 'WINDOW' MODEL - ELASTIC CONDITIONS

Figures 2 and 3 reveal from a longitudinal and transverse view the areal extent of the window.

Figure 2 shows that the window consists of 14 joints on strike and 24 limbs down dip resulting in a total of (14 x 24 x 25) 8400 elements with individual element dimensions of 6.09 m on strike and 3.05 m down dip which is also the smallest pillar size that can be modelled.

The boxhole pillars are slightly larger than this with an average dimension of 5.5 m on strike and 4.6 m down dip. This would mean that the actual stresses indicated by the model would be about 20-25% higher than the actual stresses experienced by the boxhole pillars themselves. In actual fact, at stresses near the yield value of a pillar the actual intact area (unspalled portion) may very well correspond to the actual model element dimensions. Consequently, the simulated boxhole pillar stresses indicated with the elastic analysis in an area at, or near, yield (as observed at the same location by mine staff) were used at their face value for an estimate of their yield strength. Also, the mined portion between boxholes was 6.09 m which is a somewhat greater span than actual.

RESULTS OF ANALYSES - ELASTIC WINDOW

Examination of the actual boxhole pillars that had failed violently for a given horizontal pillar was used to obtain the estimate of failure strength of an element. Close inspection suggested that for the unconfined boxhole pillar a value of 100 MPa approximated very well to its failure strength.

Figure 8 indicates that on the 602 and 702 levels on the eastern extremity there are high stress conditions at, or near, yield.

The 806E pillar shows possible yield values exceeded at the west and east extremities.

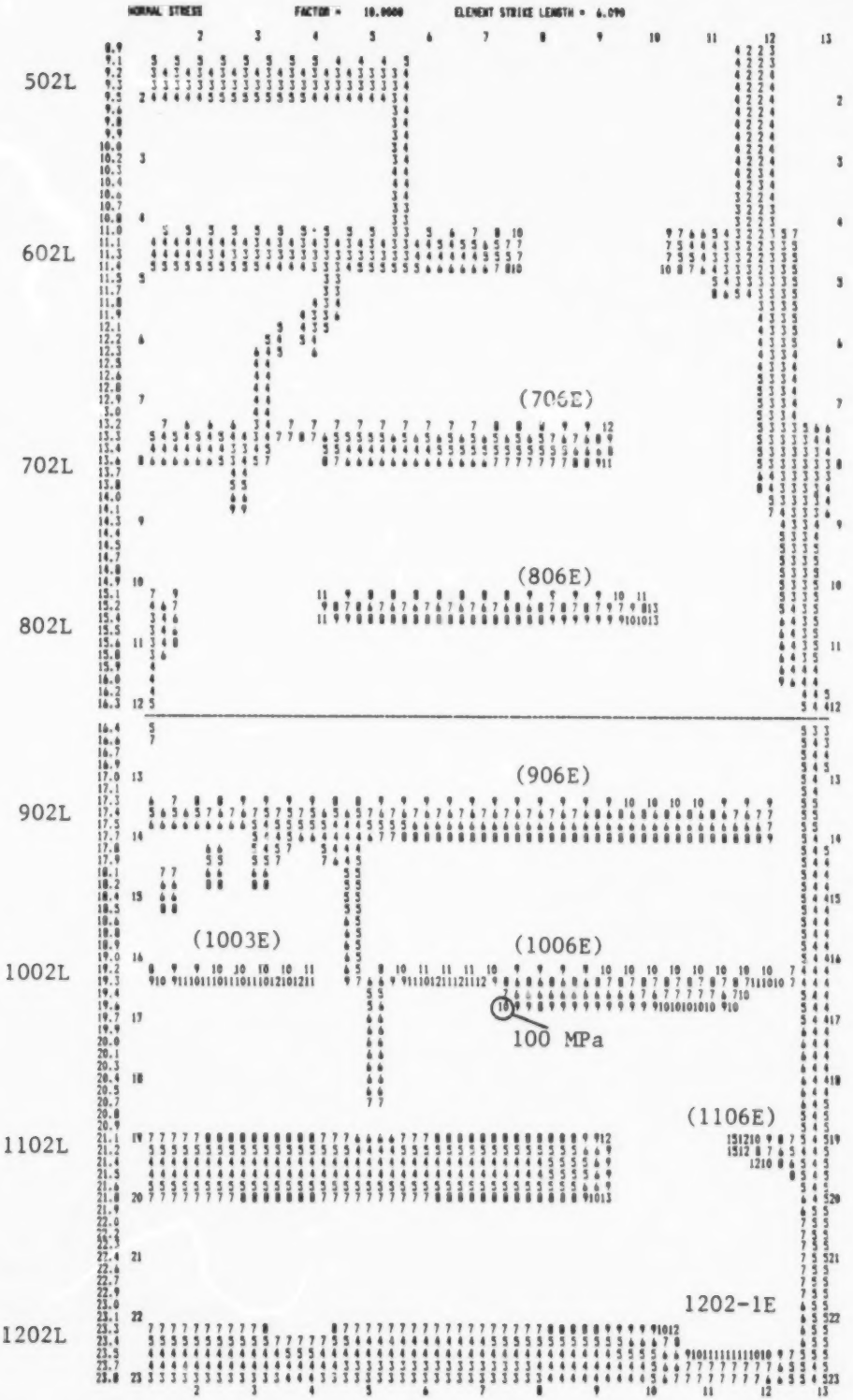

Fig. 8 - Elastic conditions, no backfill - normal stress, window "A" zone.

The 906E pillar shows the boxhole pillars at the eastern end at, or approaching the 100 MPa criterion, and the 1003E pillar indicating a possible yield condition throughout. The 1006E pillar reveals near yield conditions at its west and east extremities with some suggestion of yield at the east end of the 1106 crown pillar as well.

The 1106E sill and crown pillar at the eastern extremity where attached to the vertical barrier pillar has perpendicular stress values at the west end exceeding 100 MPA, but the larger pillar further to the west does not indicate a similar response.

The 1202-1E crown pillar above the 1402-1 backfilled stope is also showing signs of high perpendicular stresses.

The convergence values (Figure 9) for the window reflect the same magnitudes as for the coarse run (Figure 6).

INTERPRETATION OF RESULTS - ELASTIC WINDOW

From 602E level through to the 1202E level several boxhole pillars (Figure 8) have perpendicular stresses that are equal to, or exceed, 100 MPA.

Where vertical rib pillars intersect the horizontal crown or sill pillars the stress conditions are reduced within these sill areas.

Most vertical pillars are more stable than their horizontal counterparts as the vertical pillar strike length exceeds the sill pillar dip width in most cases.

High stress conditions equal to or exceeding 100 MPa are present , not only within the boxhole pillars at the east and west extremities, but also within the crown portions of these same pillars.

Based on perpendicular stress levels alone it appears that the two historically recorded failure patterns mentioned previously are suggested. For example, thin sill (boxhole) and crown pillars completely isolated from the parent rock mass (Figure 8, 806E) suggest the first failure growth pattern

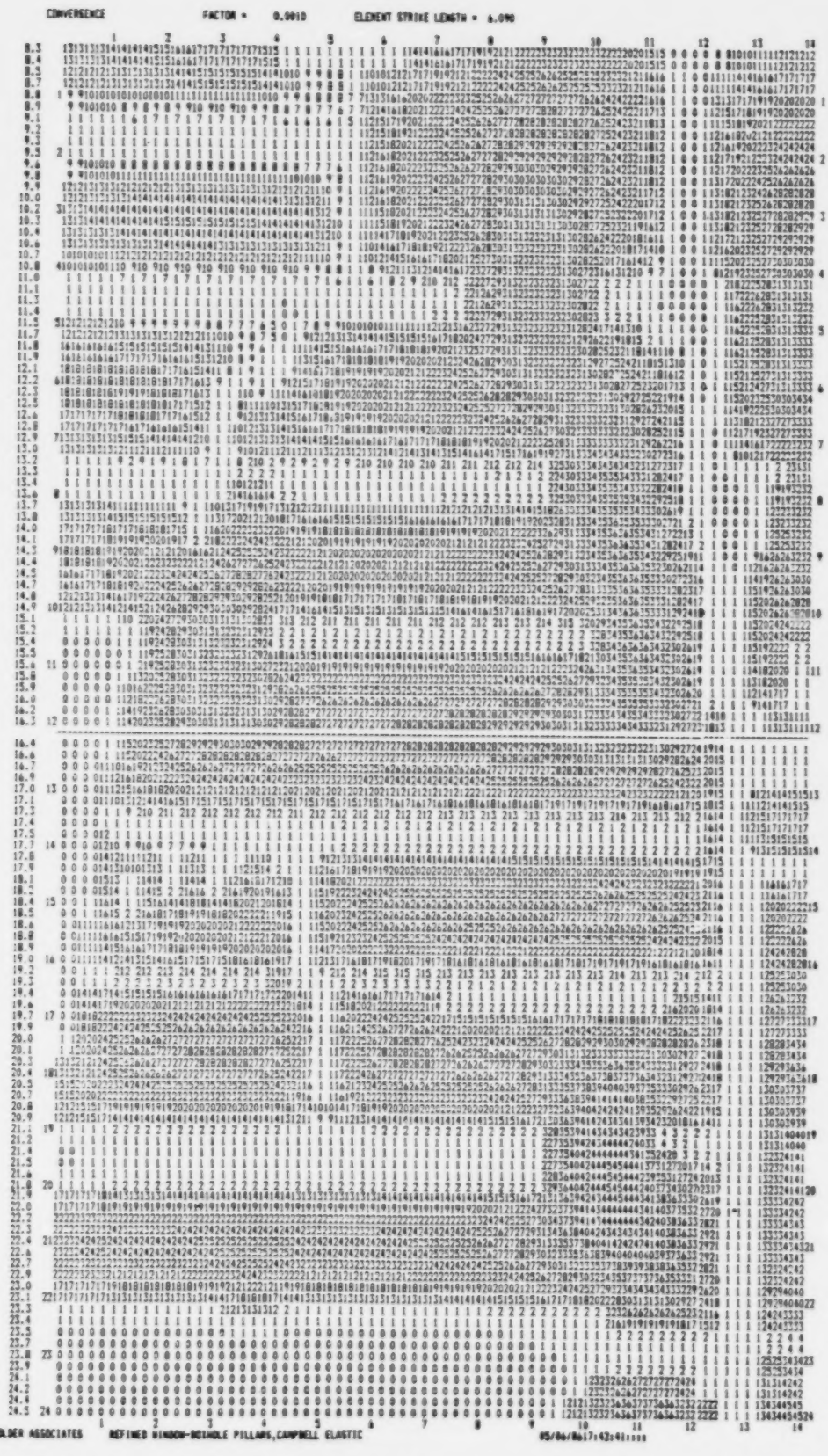

Fig. 9 - Elastic conditions, no backfill - convergence window, "A" zone.

(i), while those sill and crown pillars attached to the parent rock mass at their west end (Figure 8, 706E) and intersected by vertical pillars, suggest the second failure pattern (ii).

The boundary pillar in general is experiencing fairly low stress conditions except where local protuberances act as stress risers.

Convergence results for the elastic window (Figure 7) agree closely with the previous results for the former coarser mine model (Figure 6).

DESCRIPTION OF THE NFOLD 'WINDOW' MODEL - YIELDING CONDITIONS

The same window mentioned in the previous section, of 14 joints on strike and 24 limbs down dip has now been modified to include the effects of confinement both on the yield strength and the residual strength of the individual elements (6.04 m on strike, 3.05 m down dip). The logic behind the load-deformation properties assigned to the elements with varying confinement (lateral confining stress) is demonstrated in Figure 10.

Elements defining the individual boxhole pillars were considered to have the lowest strength (material reference No. 12), followed by those elements forming the immediate stope back representing the bottom of the crown pillar (material reference No. 22). Those elements confined on three sides by neighbouring elements directly below the mined element between boxholes (material reference No. 32) were considered the next strongest. Elements with further confinement (material reference Nos. 42 and 52, etc.) were assigned higher values yet. For those elements which were confined to an even higher degree these were assigned linearly elastic properties which would suggest intact rock conditions.

Table 3 gives the seam material thickness and properties along with the more detailed unmined, or partially 'mined' seam material average properties.

No contribution effects of backfill were included for some of the lower

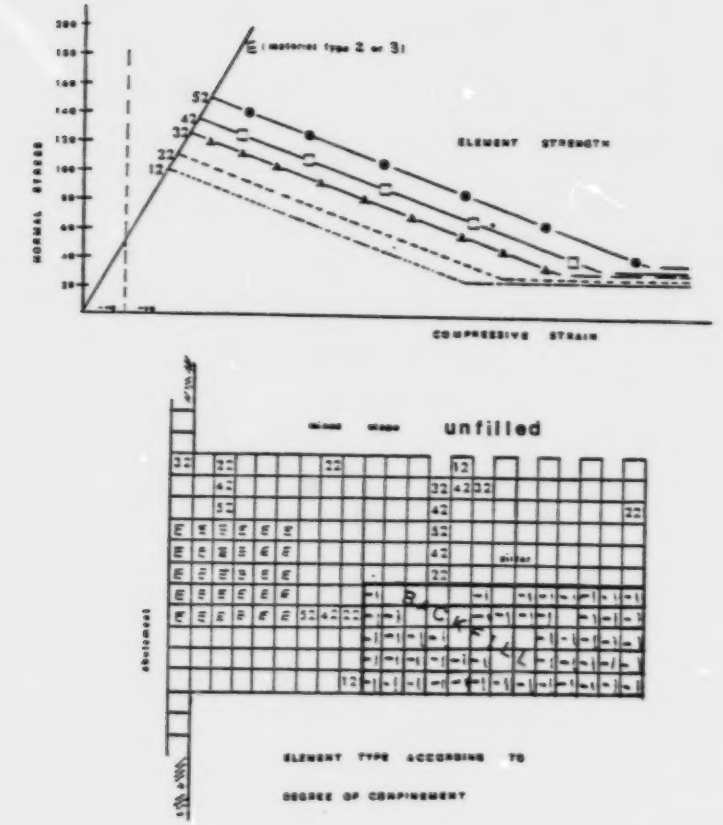

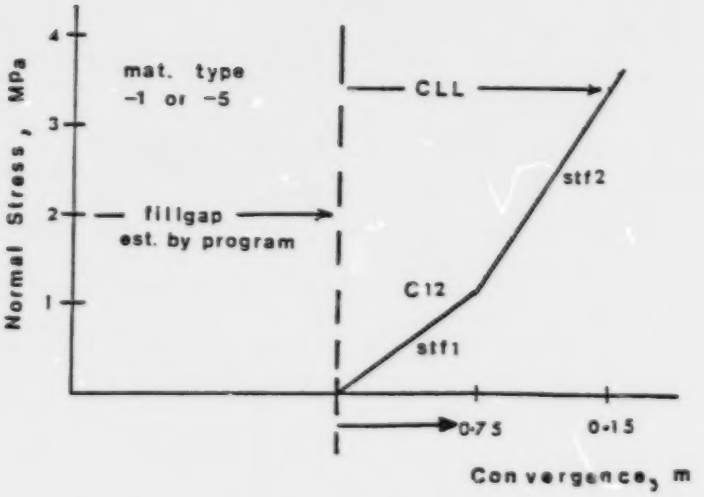

BACKFILL RESPONSE

Fig. 10 - Load deformational behaviour of the various yielding elements c/w backfill elements assigned to the NFOLD model.

stopes containing fill (below the 1002 level).

Figure 11 shows the perpendicular stresses and mining pattern layout incorporating the yielding elements.

RESULTS OF THE ANALYSES - YIELDING WINDOW

Figure 12 reveals both the mining pattern layout, factor of safety, and the failed elements within the defined window.

As suggested previously some failure of the eastern extremity of the 606, 706E sill pillars is noted. The eastern half of the 806E sill and boxhole pillar geometry has failed with some initiated failure starting in the western extremity. The 906E boxhole pillars on the eastern half have failed. The 1002E sill and boxhole pillars and a good majority of the 1006E boxhole and sill pillar geometry has failed except for a confined core which is highly stressed. The 1106E sill has failed elements both at the eastern extremity and the protuberance west of the boundary rib pillar. The 1202-1E sill above the 1402-1E stope has some failed elements present as well.

Examination of Figure 11 shows that for all failed elements the residual stress conditions are present.

Comparisons between Figures 9 and 13 show that incorporating post failure elements representing the actual boxhole pillars versus elastic elements resulted only in a slightly greater convergence in those areas where no failure (of boxholes) takes place. Examples are the 806E and 906E boxholes where 12mm to 13 mm represented convergence between boxhole pillars using post failure elements versus 11 mm and 12 mm using elastic elements.

Where failure has taken place the relative convergence change has been somewhat more dramatic. Again as an example the 906E failed boxhole pillars produced an average convergence of 14 mm and 16-17 mm between pillars. This compares with the elastic results of 2 mm for the boxhole pillars and 13 mm for the span between the pillars. The indication is that only a marginal

Table 3 - Load/deformation properties - "A" and "A-1" zone (backfill included)

Material Reference No.	Seam Thickness (m)	Modulus of Deformation (MPa)	Poisson's Ratio	Post Peak Deformation Modulus (MPa)	Yield Strength (MPa)	Residual Strength (MPa)	Cohesion (MPa)	Internal Angle of Friction (degrees)	Convergence Limit (m)	STF1 (1st Stage Fill Stiffness MPa/m)	Gap (Unfilled Gap) (m)	C12 (Convergence of Stiffness Change m)	STF2 (2nd Stage Fill Stiffness MPa/m)
2	2.0	69000	0.2										
3	2.0	69000	0.2										
12	2.0	69000	0.2	23000	100	25.0	50	60					
22	2.0	69000	0.2	23000	110	27.5	50	60					
37	2.0	69000	0.2	23000	125	31.25	50	60					
42	2.0	69000	0.2	23000	135	33.75	50	60					
52	2.0	69000	0.2	23000	150	37.50	50	60					
-1	(fill element "A" zone)								0.15	15.0	0.0	0.08	30.0
-5	(fill element "A-1" zone)								0.15	15.0	0.0	0.08	30.0

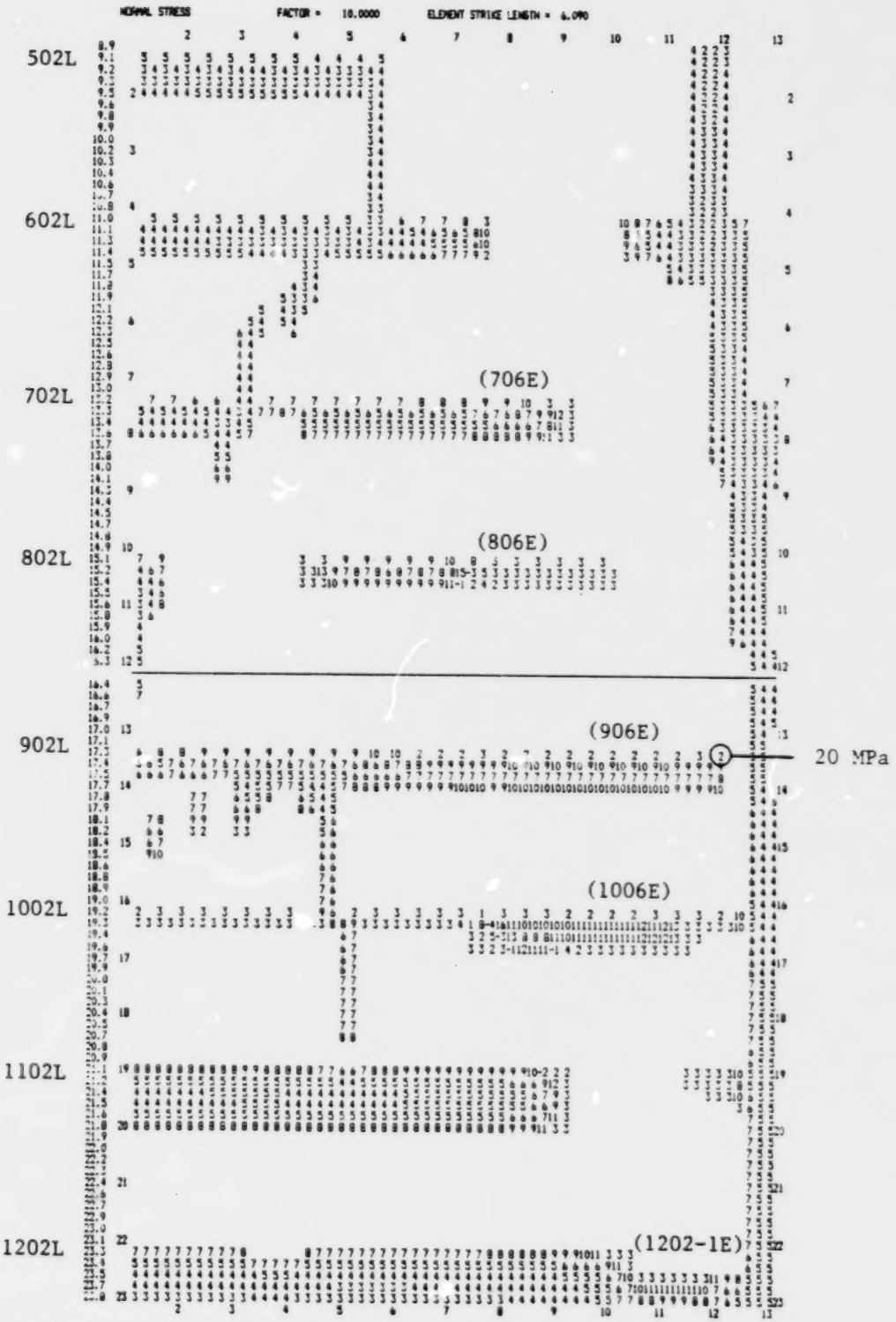

Fig. 11 - Yielding conditions, no backfill - normal stresses, window "A" zone.

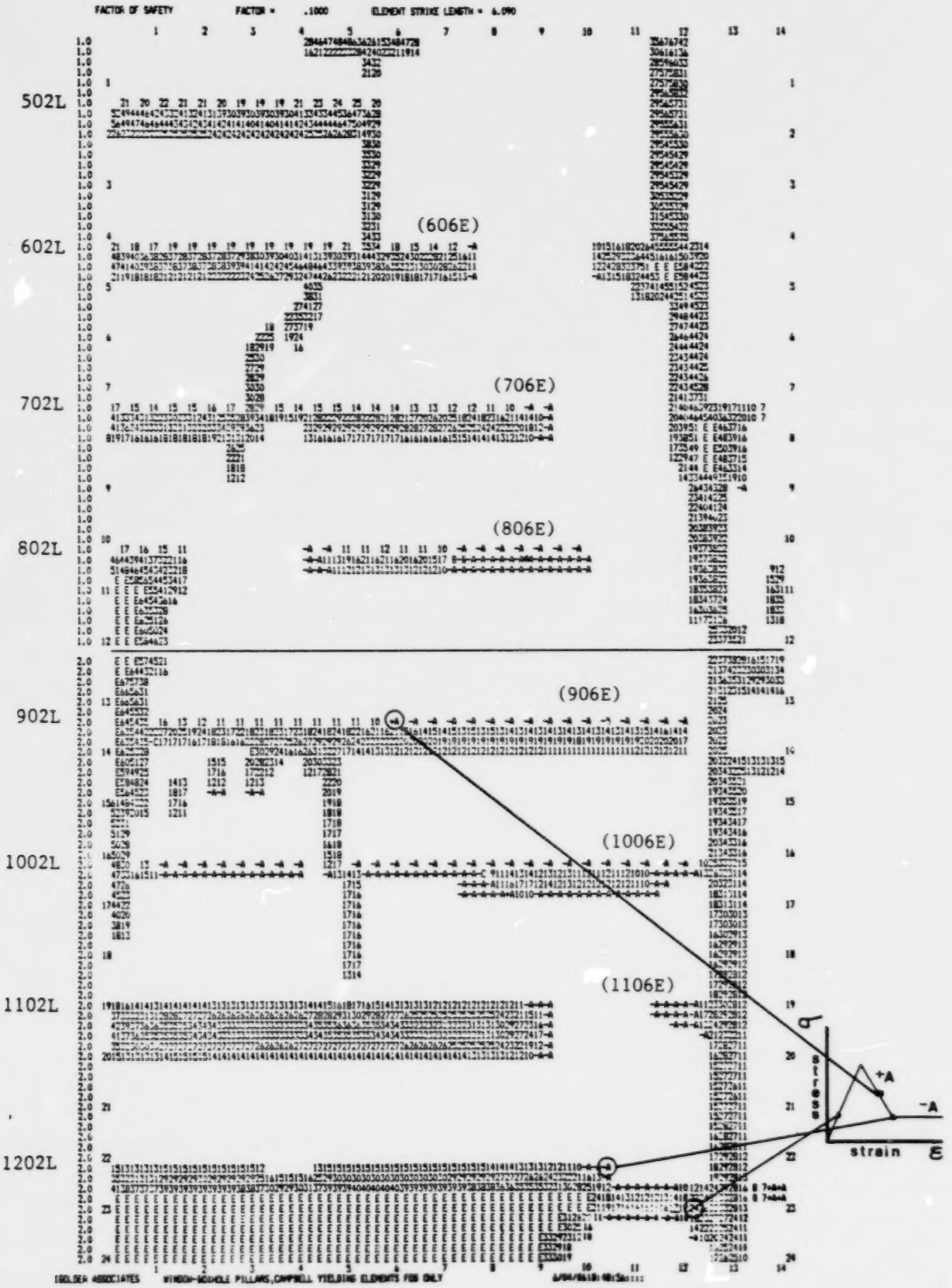

Fig.12- Yielding conditions, no backfill - factor of safety, window, "A" zone.

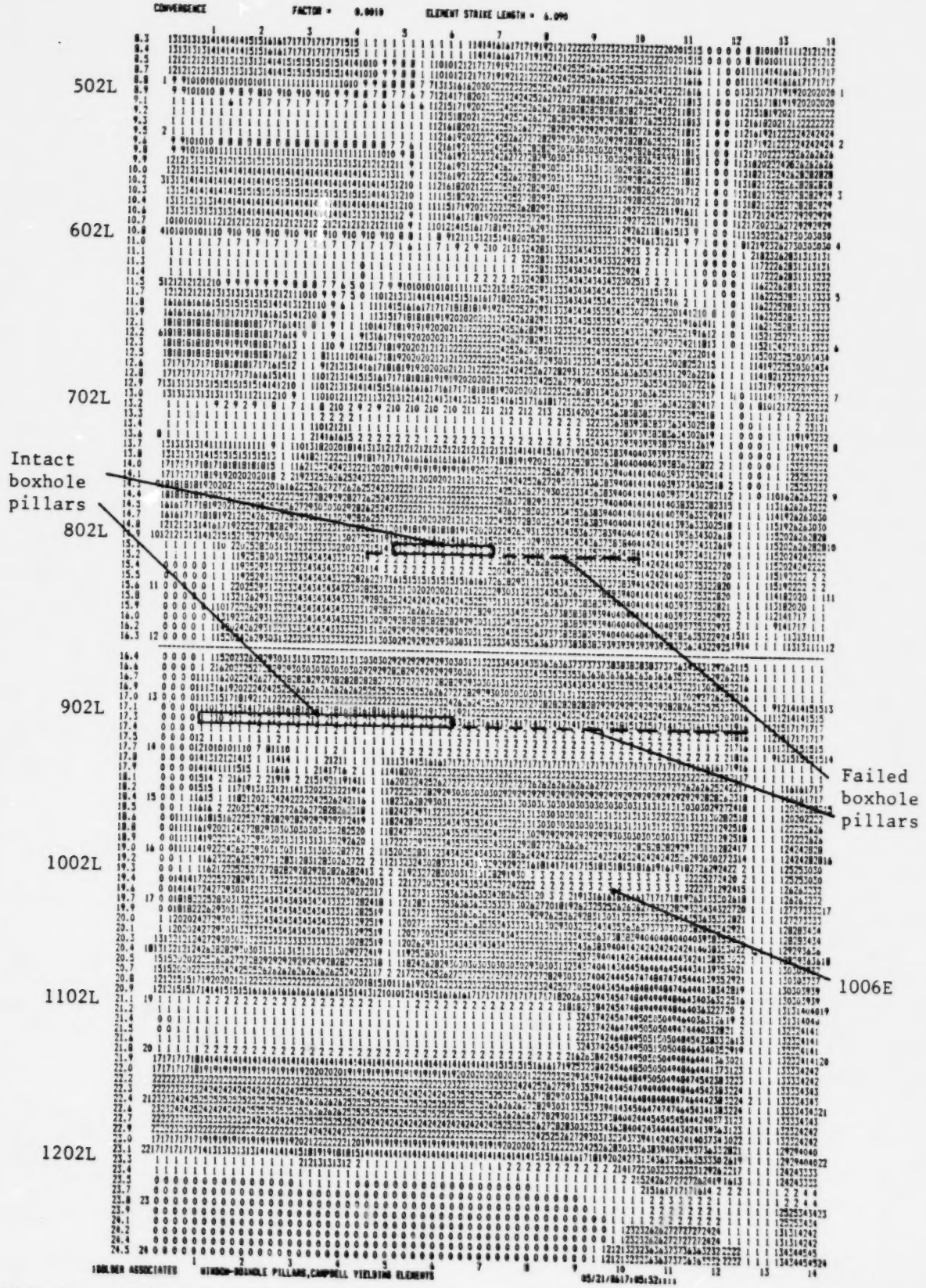

Fig. 13 - Yielding conditions, no backfill - convergence window "A" zone.

increase in convergence between pillars occurs, while a much more dramatic convergence increase occurs at the boxhole pillar locations (2 mm versus 14 mm).

At the midspans of the former mined out stopes the presence of post failure elements has caused only marginal increase in convergence. The following are location comparisons:

Stope (Midspan)	Elastic Convergence (mm)	Yielding Convergence (mm)
602E (Joint 2.5, Limb 3.5)	15	15
902E (Joint 7.0, Limb 12.5)	28	31
1102E (Joint 3.0, Limb 17.5)	28	34
1102L (Joint 10.5, Limb 19.5)	44	50

In general where fairly extensive failure has occurred there has been a substantial increase in convergence, both locally and at the midspans of the stopes as well. The increase in general has an order of magnitude of 10% or greater where failure of boxholes and/or sill pillars has taken place.

Figure 12 reveals that for most boxhole pillars below the 702 level, only a marginal factor of safety is generally present. The suggestion is that once failure occurs in a particular boxhole pillar the propagation of failure is an 'on-going' one. It also suggests that continued mining of a small tonnage of ore could also instigate an extensive propagation of failure mechanism. The sill, crown, or boxhole pillars within the 'window' area have much lower factors of safety than the vertical pillars.

Failure is indicated by the model for the western end of the 1002E sill pillar boxhole area even though the historical records to date have not shown

this area as having failed violently. The NFOLD model does not differentiate between violent and non-violent pillar failure so it is believed that the NFOLD model even though if adequately calibrated might always indicate a more extensive degree of failure than witnessed by mine personnel.

INTERPRETATION OF RESULTS - YIELDING WINDOW

The historical failure patterns described previously have been somewhat reproduced if one examines Figure 12. The 806E pillar suggests the one common failure mechanism where the east and west extremities fail first followed by the central core. This appears to be the case for the 1006E pillar as well east of the small vertical rib pillar intersection where the sill pillar is quite thin.

The other failure mechanism of initial failure of the east extremity followed by a propagation to the west holds true for those crown pillars (906E, 706E, 606E 1106E) that are attached to the west abutment.

The model indicates that in general the boxhole-crown pillars are in a meta-stable condition, and that initiation of failure caused by mine extraction even in a minute sense, or the time decay yielding of a boxhole pillar could instigate a propagation of failure that would more than likely be quite instantaneous. This has been somewhat verified by the rockbursts documented during 1986. Events 31-38 and 51-56 have occurred in reasonably rapid succession. The window geometry also suggests that stress transfers up dip to yet failed crown pillars may be sufficient to generate further failure as these pillars are approaching yield, and a greater number of events have occurred in the upper levels of the mine in 1986 (Figure 1).

The presence of yielding elements versus elastic elements results in only marginal increases in convergence in mined areas where failure is not observed. Where failure is observed fairly substantial convergence is noted both in the immediate vicinity of the failure, and at further away midspans

of previously mined stopes. This suggests that not only can the boxhole pillars fail instantly, but that it is possible that a fairly rapid change in potential energy of the wall rocks could be generated simultaneously as well.

DESCRIPTION OF THE COARSE NFOLD MINE MODEL AND WINDOW INCORPORATING BACKFILL

Examination of Figure 2 shows the overall areal extent of the coarse mine model with backfill elements included in the mined stoping blocks.

The procedure in incorporating backfill involved initially replacing the mined elements below the 1002 level in the previous elastic coarse mine model data file with backfill elements. Any elastic analysis carried out at this time would be insensitive to loading within backfill.

A window within the coarse elastic backfill model was then created with again no response accountable for the presence of backfill.

Post failure characteristics were then assigned to unmined elements within the window along with the previous load-deformational characteristics of the backfill elements. The 'window' of the backfill model was not identical to the former but was some two limbs longer down dip so that it included a greater portion of the 1402-1 cut and fill stope.

The various elements used in the 'window' numerical analyses are described (Figure 10, Table 3). The unmined yielding load-deformational behaviour of ore elements is shown along with a proposed response of the backfill elements as stope wall closure occurs. Properties of the backfill were taken from the literature (4).

RESULTS OF THE ANALYSES - WINDOW

Post failure elements form the mining pattern layouts shown in Figures 14, 15 and 16 containing backfilled elements and reflecting the slightly larger window in the down dip direction.

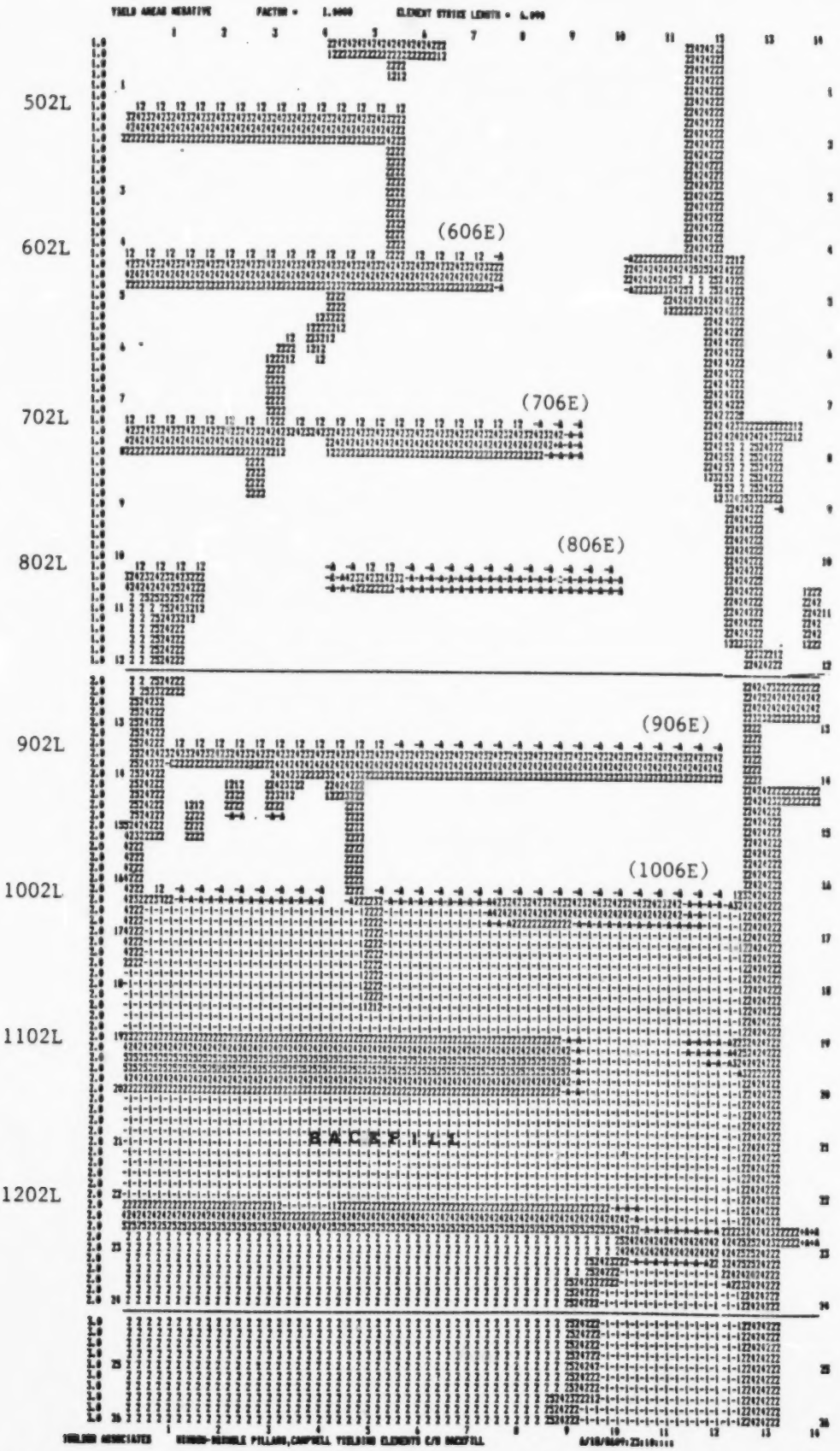

Fig. 14 - Yielding conditions with backfill - mining pattern yield areas, window "A" zone.

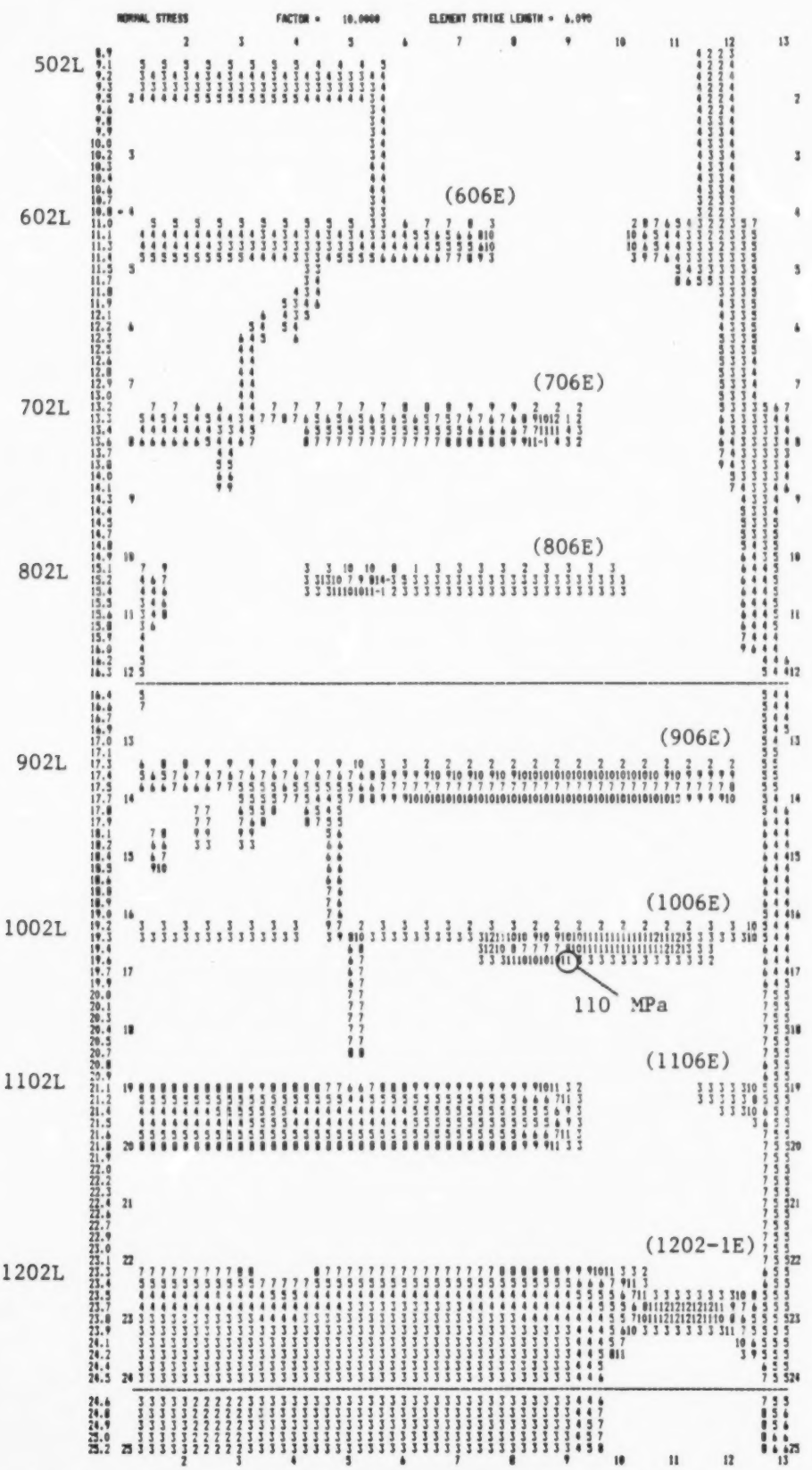

Fig. 15 - Yielding conditions with backfill - normal stresses, window "A" zone.

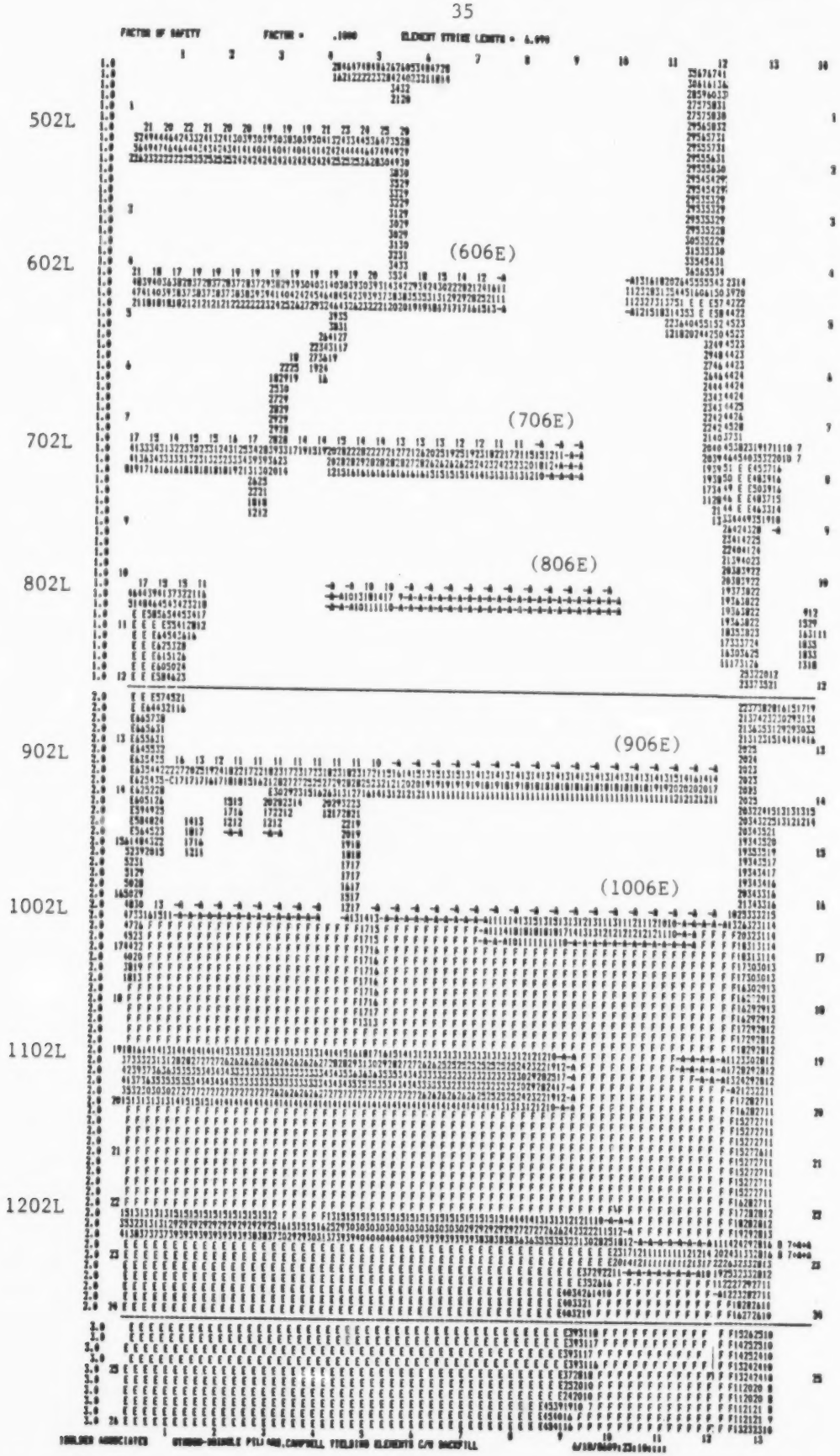

Fig. 16 - Yielding conditions with backfill - factor of safety, window "A" zone.

Although, in general, the yield area patterns for backfilled window versus the window containing no backfill are similar (Figure 12 versus Figure 16) there are some subtle differences:

a) the eastern extremity of the 706E pillar shows 6 more elements having failed than the previous case where backfill was not included.

b) the 806E boxhole and crown pillar also shows considerably more elements having failed than the previous case with no backfill.

c) the 1006E sill pillar has several more unmined elements intact than in the previous case where no backfill was present.

d) for the 1106E sill piilar the backfill has only provided a very slight increase in stabilization.

e) the 1402-1 crown pillar appears to have slightly more failed elements for the backfilled case than without the presence of backfill.

The normal stress printouts (Figures 15 and 11) also indicate a greater presence of residual stresses in the 706E and 806E pillar areas, a greater presence of intact but near yield stresses for 1006E pillar and very little change in stress results for the 1102 pillar. The 1402-1E crown pillar shows a slightly greater presence of residual stress conditions for the backfilled case than that without fill which is questionable.

Figure 16 shows that the factor of safety for unmined elements in 706E and 806E pillars near the indicated failure areas are near unity. As more iterations were run in the backfill model than the model without fill it is likely that more failure was generated due to this fact alone.

Comparisons of convergence of the 'window' with and without backfill with the fill properties used, generally indicate very little, if no, influence on the closure between walls. In the model, mass filling was used (as well as mass mining to the present geometry) so the incremental effect of filling was not truly accounted for, even though the load-deformational

backfill response used was that actually measured in a Coeur d'Alene mine. Figure 17 in comparison with Figure 13 did incorporate post failure properties for the highly stressed elements, and with backfill present should have resulted in reduced convergence of the walls in those areas. With fill the convergence near the failed elements in small sill pillars was considerably less than the same locations without. This suggests that in nearly failed areas that the fill has played a more constrained role absorbing some wall closure. The 1006E sill pillar near its bottom extremity (mined out elements just below) demonstrates this.

Examination of the 1006E sill pillar in Figures 12 and 16 show the positive contribution of backfill confinement. Not only are there less failed elements, but the factors of safety for the elastic pre-yield elements are slightly higher with backfill than without. The increase is anywhere from zero to 50% depending on the location. Where the degree of failure at other locations is less extensive very little increase in the factor of safety occurs for the elastic pre-yield elements.

INTERPRETATION OF THE RESULTS FOR MODELS INCORPORATING BACKFILL

Examination of the "A" zone geometry with, and without, backfill indicates that near the centres of the spans of mined-out openings very little reduction in closure occurs with stopes containing backfill versus no backfill. This can only be verified if yielding load-deformational properties are assigned to unmined elements.

There are some reductions in closures with backfill elements near failed pillars versus the same locations without fill. The reduction in closure, however, is not that dramatic.

The presence of fill has no effect on stress conditions in unmined elements if an elastic analysis is considered as these elements are not

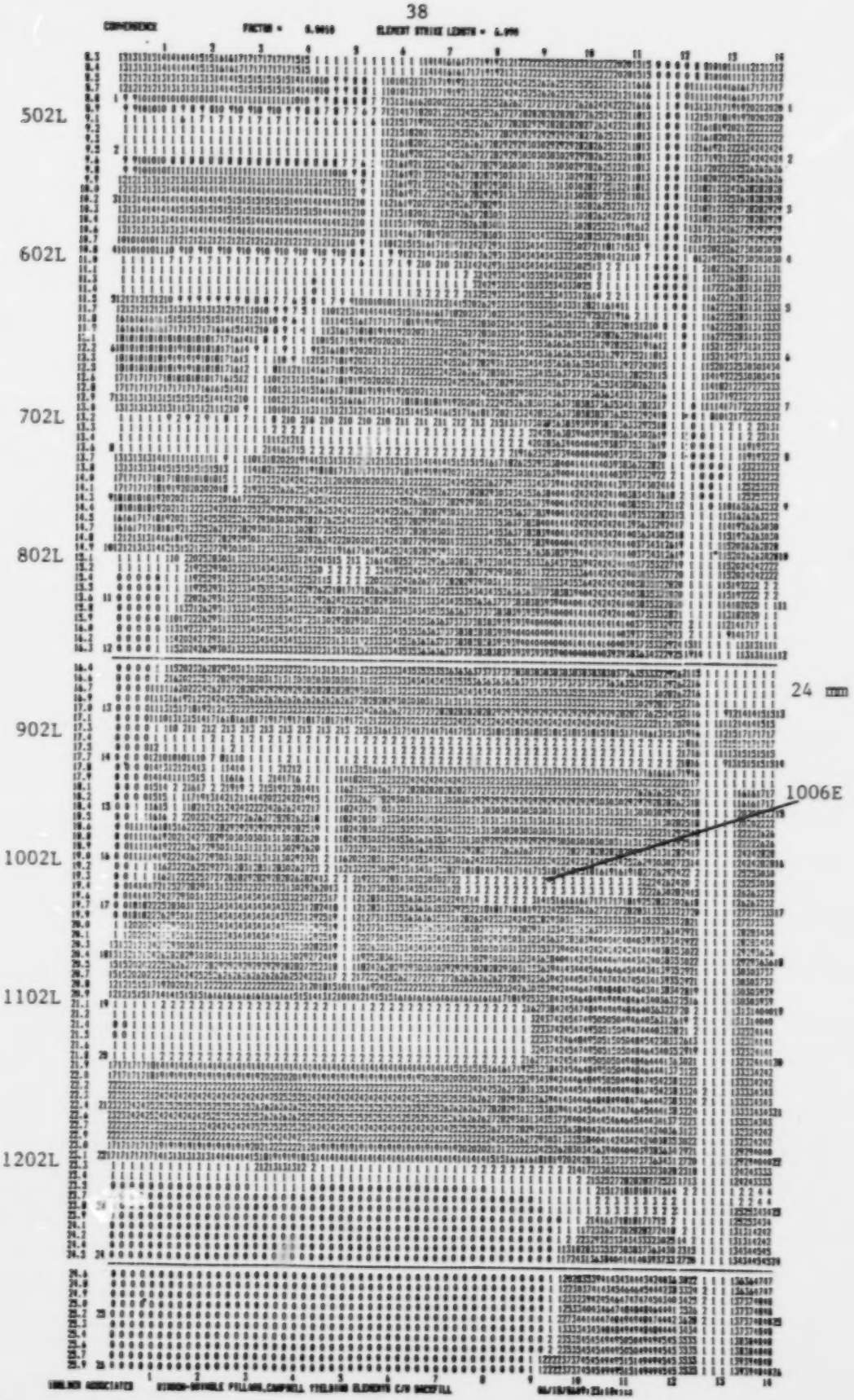

Fig. 17 - Yielding conditions with backfill - convergence, window "A" zone.

allowed to fail. However, it appears that when post-failure elements are used in the analysis, the backfill in combination with failed elements provides sufficient confinement to strengthen some elements in a pillar that would normally fail without backfill. With less elements failing with backfill present, there are more elastic pre-yield elements to bear the mining induced stresses resulting in increased factors of safety. Consequently, there could be more elastic pre-yield high stress elements in a pillar with backfill present versus less without fill.

In many sill pillar locations a marginal factor of safety (slightly greater than 1.0) for many elements is present. This indicates for the most part an extremely meta-stable condition where failure of one element in a series due to a local burst, drilling and scaling, or a small development blast, might cause a chain reaction of bursting to occur throughout the pillar.

An unexpected development incorporating backfill within the 'window' area was a greater failure pattern generated in the 706E and 806E sill and boxhole pillars. It is suspected that as more iterations were run in the backfill case than that without fill, that a greater readjustment of stresses took place causing more unmined elements to fail. Again, with a great number of unmined elements having a factor of safety near unity, even a small increase in iterations could cause this effect.

MINE STIFFNESS

Another factor to consider is the overall mine stiffness of the "A" zone. In the literature (5) O'Hearn (1968), and others (6), have indicated that as the extraction ratio increases the hanging wall/footwall mine stiffness is reduced considerably (the negative slope of the hanging wall/footwall load deformation curve becomes flatter). With the high

extraction observed above the 1102 level it would appear that the "A" zone probably has a low mine stiffness. This factor combined with the brittle response of a steeply inclined post failure curve of an unconfined boxhole pillar will generally result in violent pillar failure. The areas that will exhibit this behaviour probably will display factors of safety near unity. A correlation is that of a uniaxial compression testing apparatus where the boxhole represents the uniaxial unconfined sample, and the loading press is represented by the hanging wall/footwall rock mass. With a low stiffness press excess energy is stored within its frame and at sample yielding, explosive failure results. This occurs as the rate of load reduction during post failure is not sufficient so that the load applied by the press still exceeds the load required by the sample to fail. The excess energy stored by the loading system can be somewhat quantified by the amount of surface area between the post deformation curve of the sample and load-deformation curve of the loading system. In the "A" zone and orebodies like it where the ore modulus is fairly high and where extraction is high rockbursts are common as a result.

A coincident factor is the time decay failure in a incremental minewide sense. Even though no mining may take place, every time a boxhole pillar fails the mine stiffness is reduced, and stress transfers to the stronger pillars occur. If the factors of safety for these stronger pillars is near unity the fact that the mine stiffness will continue to reduce almost guarantees the possibility of further pillar bursting. Eventually, when all low strength remnants have failed and the stresses have transferred to the abutments, then the mine geometry is once again stable.

CONCLUSIONS

1. The NFOLD numerical method is a reasonably accurate model in simulating mining induced stresses transferred to yet unmined remnants. This is particularly true where the ore seam to be modelled is thin in relation to its other dimensions.

2. The NFOLD numerical results suggest that the two main failure patterns (Figure 12, i.e., 806E versus 906E, 1106E, 606E, etc.) witnessed in the "A" zone in the past are for the most part implied by the model. Most areas predicted by the model as having failed have failed, but there are other areas predicted where no yielding has been observed by mine personnel in a 'violent rockburst' sense.

   It is possible in this case, that non-violent failure may have occurred and gone unnoticed. Failure growth in a mine-wide sense was not verified as successive mining steps were not introduced to attempt to initiate failure at a particular location and let it proceed from there. Choosing the initial location would be difficult.

3. Both elastic runs on the coarse mine model and yielding load-deformational behaviour on the 'window' model suggest that several sill and boxhole pillar combinations are highly stressed, and are in a meta-stable condition. This is true for both the Campbell "A" zone as well as the very small sill remnants on the Dickenson Mine side of the vertical boundary pillar. This suggests possible chain reaction effects and an affinity for rockbursts to occur in fairly rapid succession along these pillars.

4. The boundary pillar separating Campbell Red Lake "A" zone from the Dickenson Mine appears to remain in an intact state (no failure) throughout its length except where local protruberances act as stress risers. The vertical pillars in general are fairly stable compared with horizontal

pillars.

5. The inclusion of the "A-1" zone with the "A" zone in the NFOLD model did show reduced normal stress shadowing within the "A-1" seam to the east of its presently active stopes.

6. When comparing elastic and yielding convergence results for the same geometry containing no backfill, the increased convergence is more spectacular in the vicinities of failed pillars than at the midspans of stopes separating these pillars. This infers that convergence is controlled by span where the relative span change for the stope is insignificant but the span change between boxholes is very dominant when a boxhole pillar fails.

7. Only when post-failure load-deformation properties are assigned to unmined elements can any backfill contribution be evaluated. It appears that the presence of fill provides confinement to those portions of pillars that have excellent potential for failure, and may prevent pillar convergence to the degree that allows failure to occur. This effect, however, is observed only in a very few cases, and for most other areas backfill does not seem to provide an increased stabilizing effect.

8. Less convergence occurs near boxhole-crown pillar combinations with backfill present than without, but the degree of convergence reduction is very slight at midspans of stopes. The above effect is most likely due to span dependancy, and the fact that the fill stiffness used in the model, although equivalent to field values, may not be high enough for the NFOLD model to adequately account for its restraint.

9. The presence of backfill providing confinement to the peripheral portions of some horizontal pillars results in higher pre-yield stresses being borne by these regions which consequently result in lower stresses in the central core of the pillar.

10. The NFOLD model appears to be reasonably well calibrated as its predictive failed regions agree well with observed failure in the mine and it implies a failure growth pattern that has also been observed to exist in the mine. If there is a shortcoming of the NFOLD model it is that it does not account for the time decay of pillars under high stresses where the factors of safety are near unity for many pillar locations throughout the mine. If the mine geometry indicates this to be the case, picking the degree of pillar failure observed at a point in time as a method of calibrating the model could be quite inaccurate. Some overdesign could be implemented by indicating failure at stresses less than the optimum which match the observed failure conditions to compensate for this shortcoming.
11. The NFOLD model can now be used to examine various mining scenarios for the unmined portions of A and A-1 zones.

ACKNOWLEDGEMENTS

The author would like to thank the management of Campbell Red Lake Lines Ltd. for permission to publish this report. I am grateful for the data received from T. Makuch, B. Arjang, D. Hedley of the Elliot Lake Research Laboratory, and to Golder Associates in the use of their NFOLD computer program.

REFERENCES

1. Hedley, D.G.F., Newmann, M., Makuch, T. and Blake, W., "Rockbursts at Campbell Red Lake Mine"; Division Report MRP/MRL 85-31(OP); CANMET, Energy, Mines and Resources Canada; 1985.

2. Hammett, R.D., "Report on results of NFOLD analyses conducted for Campbell Red Lake Mines Ltd., Balmertown, Ontario"; Company Report, Golder Asociates, Vancouver, B.C.; 1985.

3. Arjang, B., "Field and pillar stress determinations at Campbell Red Lake Mines, Ontario"; Division Report M&ET/MRL 86-57(TR); CANMET, Energy, Mines and Resources Canada; 1986.

4. Corson, D.R. and Wayment, W.R., "Load-displacement measurement in a backfilled stope of a deep vein mine"; Report of Investigations RI 7038, U.S. Bureau of Mines; 1967.

5. O'Hearn, B., "The development and use of computer models to determine wall stiffness in a bord and pillar layouts"; M.Sc. Thesis, Univerity of Witwatersrand, Johannesburg, S. Africa; 1985.

6. Jaeger, J.C., Cook, N.W.G., "Fundamentals of rock mechanics"; Chapman and Hall Ltd., Chapter 18.6, pp 454-458; 1969.